arXiv:1605.00116v3 [hep-ex] 14 Oct 2016

Measurement of the integrated and differential $t\bar{t}$ production cross sections for high-p_T top quarks in pp collisions at $\sqrt{s} = 8$ TeV

The CMS Collaboration[*]

Abstract

The cross section for pair production of top quarks ($t\bar{t}$) with high transverse momenta is measured in pp collisions, collected with the CMS detector at the LHC with $\sqrt{s} = 8$ TeV in data corresponding to an integrated luminosity of 19.7 fb^{-1}. The measurement is performed using lepton+jets events, where one top quark decays semileptonically, while the second top quark decays to a hadronic final state. The hadronic decay is reconstructed as a single, large-radius jet, and identified as a top quark candidate using jet substructure techniques. The integrated cross section and the differential cross sections as a function of top quark p_T and rapidity are measured at particle level within a fiducial region related to the detector-level requirements and at parton level. The particle-level integrated cross section is found to be $\sigma_{t\bar{t}} = 0.499 \pm 0.035\,\text{(stat+syst)} \pm 0.095\,\text{(theo)} \pm 0.013\,\text{(lumi)}$ pb for top quark $p_T > 400$ GeV. The parton-level measurement is $\sigma_{t\bar{t}} = 1.44 \pm 0.10\,\text{(stat+syst)} \pm 0.29\,\text{(theo)} \pm 0.04\,\text{(lumi)}$ pb. The integrated and differential cross section results are compared to predictions from several event generators.

[*]See Appendix A for the list of collaboration members

1 Introduction

Measurements of top quark pair ($t\bar{t}$) production cross sections provide crucial information for testing the standard model (SM) and the accuracy of predictions from Monte Carlo (MC) generators. The CMS [1] and ATLAS [2] Collaborations at the CERN LHC have previously measured the differential $t\bar{t}$ cross sections at $\sqrt{s} = 7$ and 8 TeV as a function of transverse momentum (p_T) and other kinematic properties of the top quarks and the overall $t\bar{t}$ events [3–9]. These measurements use events where each parton from the top quark decay is associated with a distinct jet. However, when top quarks are produced with large Lorentz boosts, their decays are often collimated and the final decay products may be merged. For a top quark with a Lorentz boost of $\gamma = E/m$, where E is the energy and m the mass of the top quark, the angle ΔR in radians between the W boson and the b quark from the top quark decay is approximately $\Delta R = 2/\gamma$. In this paper, a measurement of the $t\bar{t}$ production cross section is presented utilizing jet substructure techniques to enhance sensitivity in the kinematic region with high-p_T top quarks. Accurate modeling of the boosted top quark regime is important as it is sensitive to many physics processes beyond the SM, as discussed, for example, in Ref. [10].

This paper presents the first CMS measurement of the $t\bar{t}$ production cross section in the boosted regime. The cross section is measured as a function of the top quark transverse momentum (p_T^t) and rapidity (y^t) for $p_T^t > 400$ GeV, corresponding to the upper p_T range covered by the CMS measurement in Ref. [4]. A dedicated measurement of $t\bar{t}$ production in the boosted regime has recently been reported by the ATLAS Collaboration [11].

The analysis is performed for events in lepton+jets final states where one top quark decays according to $t \to Wb \to \ell\nu b$, with ℓ denoting an electron or a muon, and the second top quark decays to quarks ($t \to Wb \to q\overline{q}'b$). Lepton+jets final states originating from W boson decays to τ leptons ($t \to Wb \to \tau\nu b \to \ell\overline{\nu}\nu b$) are treated as background. The boosted top quark that decays to a hadronic final state is reconstructed as a single, large-radius (large-R) jet. Jet substructure techniques similar to those used in Refs. [12, 13] are applied to identify those large-R jets originating from top quarks (t-tagged jets). A maximum-likelihood fit is performed to extract the background normalizations, the t tagging efficiency, and the integrated $t\bar{t}$ production cross section for $p_T^t > 400$ GeV. The results are presented at the particle level in a fiducial region similar to the event selection criteria to minimize the dependence on theoretical input, and fully corrected to the parton level. Differential $t\bar{t}$ cross sections are also measured at the particle (parton) level as a function of the t-tagged jet (top quark) p_T and y after subtracting the background contributions and correcting for inefficiencies and bin migrations.

2 The CMS detector, event reconstruction, and event samples

The CMS detector [1] is a general-purpose detector that uses a silicon tracker, a finely segmented lead tungstate crystal electromagnetic calorimeter (ECAL), and a brass and scintillator hadron calorimeter (HCAL). These subdetectors have full azimuthal coverage and are contained within the bore of a superconducting solenoid that provides a 3.8 T axial magnetic field. Charged particles are reconstructed in the tracker, covering a pseudorapidity [1] range of $|\eta| < 2.5$. The surrounding ECAL and HCAL provide coverage for photon, electron, and jet reconstruction for $|\eta| < 3$. Muons are measured in gas-ionization detectors embedded in the steel flux-return yoke outside the solenoid. Events are reconstructed using the particle-flow algorithm [14, 15], which identifies each particle with an optimized combination of all subdetector information. The missing transverse momentum vector $\vec{p}_T^{\text{miss}}$ is defined as the projection on the plane perpendicular to the beams of the negative vector sum of the momenta of

all reconstructed particles in an event. Its magnitude is referred to as $E_{\mathrm{T}}^{\mathrm{miss}}$. A more detailed description of the CMS detector, together with a definition of the coordinate system used and the relevant kinematic variables, can be found in Ref. [1].

The measurement is performed using the CMS data recorded at $\sqrt{s} = 8\,\text{TeV}$, corresponding to an integrated luminosity of $19.7 \pm 0.5\,\text{fb}^{-1}$ [16]. For the e+jets channel, data are collected with a trigger requiring an electron with $p_{\mathrm{T}} > 30\,\text{GeV}$ and $|\eta| < 2.5$, at least one jet with $p_{\mathrm{T}} > 100\,\text{GeV}$, and at least one additional jet with $p_{\mathrm{T}} > 25\,\text{GeV}$. For the μ+jets channel, the trigger demands a muon with $p_{\mathrm{T}} > 40\,\text{GeV}$ and $|\eta| < 2.1$, with no jet requirements. At the trigger level, the leptons are not required to be isolated.

Simulated events are used to estimate the efficiency to reconstruct the $t\bar{t}$ signal, evaluate the systematic uncertainties, and model most of the background contributions. Samples of $t\bar{t}$ and electroweak single top quark events are generated using the next-to-leading-order (NLO) MC generator POWHEG (v. 1.0) [17–21], while W boson production in association with jets is generated with the leading-order (LO) generator MADGRAPH (v. 5.1.3.30) [22]. Additional $t\bar{t}$ samples, generated using MADGRAPH and the NLO generator MC@NLO (v. 3.41) [23], are used for comparison with POWHEG. The MC@NLO production is interfaced to HERWIG (v. 6.520, referred to as HERWIG6 in the following) [24] for parton showering, while all other generators are interfaced to PYTHIA (v. 6.426, referred to as PYTHIA6) [25]. For the samples produced with MAD-GRAPH, the MLM prescription [26] is applied for matching of matrix-element jets to parton showers. The most recent PYTHIA Z2* tune is used. It is derived from the Z1 tune [27], which uses the CTEQ5L parton distribution function (PDF) set, whereas Z2* adopts CTEQ6L [28]. The POWHEG $t\bar{t}$ and single top quark samples are generated using the CT10 next-to-next-to-leading-order (NNLO) [29] PDFs, while the MC@NLO $t\bar{t}$ sample uses the NLO CTEQ6M [28] PDF set. The LO CTEQ6L1 [28] PDF set is used for the MADGRAPH $t\bar{t}$ and W+jets samples. All generated events are propagated through a simulation of the CMS detector based on GEANT4 (v. 9.4) [30].

The simulated events are corrected to match the conditions observed in data. All simulated events are reweighted to reproduce the distribution of the number of primary vertices that arises from additional pp interactions within the same or neighboring bunch crossings (pileup), as measured in data. The jet energy resolution is corrected by scaling the difference between the generated and the reconstructed jet momentum so that the resolution matches that observed in data [31]. Lepton trigger and identification efficiencies are also corrected for differences between data and simulation. Jet energy corrections are obtained from the simulation and further corrections are applied to data from in situ measurements using the energy balance in dijet and photon+jet events [31]. The contribution to the jet energy in data from pileup is removed using the area-based subtraction technique outlined in Ref. [32], augmented by corrections from data as a function of the jet η, as described in Ref. [31].

3 Event selection

Jet clustering is performed with the FASTJET package (v. 3.1) [33]. Two jet clustering algorithms are used in the measurement. The anti-k_{T} algorithm [34] with a distance parameter $R = 0.5$ is used to reconstruct jets that are hereafter referred to as small-R jets. Lepton candidates that are found within $\Delta R < 0.5$ of a jet, where $\Delta R = \sqrt{(\Delta\eta)^2 + (\Delta\phi)^2}$ and $\Delta\eta$ and $\Delta\phi$ are the pseudorapidity and azimuthal angle (in radians) differences between the direction of the lepton and the jet, are subtracted from the jet four-vector to avoid including such leptons within jets. The small-R jets are required to have $p_{\mathrm{T}} > 30\,\text{GeV}$ and $|\eta| < 2.4$. Small-R jets that are iden-

tified as originating from a bottom (b) quark through the use of an algorithm that combines secondary-vertex and track-based lifetime information [35, 36] are classified as being b tagged. The algorithm working point used has an efficiency for tagging a b jet of $\approx$65%, while the probability to misidentify light-flavor jets as b jets is $\approx$1.5%. The secondary-vertex mass of the b-tagged jet (m_{vtx}) is defined as the invariant mass of the tracks associated with the secondary vertex, assuming that each particle has the pion mass. Jets that are b tagged are also required to have a secondary vertex (resulting in a small change in the efficiency). Differences in b tagging efficiency and misidentification rates between data and simulated events are accounted for through scale factors applied to the simulation.

The second jet clustering algorithm is the Cambridge–Aachen (CA) algorithm [37, 38], used to reconstruct large-R jets with a distance parameter $R = 0.8$. These jets are required to have $p_{\mathrm{T}} > 400$ GeV, where this lower p_{T} bound is set such that the top quark decay products are typically fully merged for $R = 0.8$. The kinematics of the large-R jet is used for the $p_{\mathrm{T}}^{\mathrm{t}}$ and y^{t} measurements.

The CMS top quark tagging algorithm [39], using large-R jets as input, is employed in this measurement to identify top quark candidates decaying hadronically. The algorithm begins by identifying subjets through recursive declustering of the original large-R jet, reversing the clustering sequence of the CA algorithm. First, the last clustering step is reversed, splitting the large-R jet j, with transverse momentum denoted as $p_{\mathrm{T}}^{\mathrm{j}}$, into two subjets j_1 and j_2, with transverse momenta $p_{\mathrm{T}}^{\mathrm{j}_1}$ and $p_{\mathrm{T}}^{\mathrm{j}_2}$. If the two subjets satisfy $\Delta R(\mathrm{j}_1, \mathrm{j}_2) > 0.4 - 0.0004\,p_{\mathrm{T}}^{\mathrm{j}}$, with $p_{\mathrm{T}}^{\mathrm{j}}$ in GeV, they are passed to the next step of the algorithm; if not, they are reclustered and the parent is labeled as a hard subjet. Each subjet is required to satisfy $p_{\mathrm{T}}^{j_i} > 0.05\,p_{\mathrm{T}}^{\mathrm{j}}$; otherwise, the subjet is discarded. A secondary decomposition is next applied to the subjet(s), identifying up to a maximum of four hard subjets.

The large-R jet that is identified as a t jet candidate is required to contain at least three subjets, corresponding to the presumed b, q, and $\overline{\mathrm{q}}'$ fragmentation products. In addition, the minimum pairwise invariant mass of the three subjets of highest p_{T} is required to be greater than 50 GeV, as expected for the $\mathrm{t} \rightarrow \mathrm{Wb}$ decay, and the total jet invariant mass m_{j} is required to be consistent with the top quark mass by demanding $140 < m_{\mathrm{j}} < 250$ GeV. Large-R jets which fulfill these requirements are labeled as t-tagged jets. The cumulative efficiency for these t tagging requirements is about 25% for $|\eta| < 1.0$ and 13% for $1.0 < |\eta| < 2.4$ [39]. The difference in the t tagging efficiency between data and simulation is accounted for through a scale factor applied to the simulation that is derived using a maximum-likelihood fit.

Electrons [40] and muons [41] must have, respectively, $p_{\mathrm{T}} > 35$ GeV and 45 GeV, and $|\eta| < 2.5$ and 2.1, where the differences are a consequence of the requirements on the respective lepton triggers. Since leptons from high-p_{T} top quark decays are often emitted close to their accompanying b jets, they may not be well-isolated. To reject background contributions from jets misidentified as leptons, the leptons must pass a two-dimensional (2D) selection, requiring either $\Delta R(\ell, \text{closest small-}R\text{ jet}) > 0.5$ or $p_{\mathrm{T}}^{\mathrm{rel}} > 25$ GeV, where $p_{\mathrm{T}}^{\mathrm{rel}}$ is the component of the lepton p_{T} perpendicular to the axis of the closest small-R jet. An additional criterion is applied in the electron channel to further reduce the multijet background contribution from mismeasured jets. The requirement ensures that $\vec{p}_{\mathrm{T}}^{\mathrm{miss}}$ does not point parallel to the direction of either the electron (e) or the highest-p_{T} jet (j) for low-$E_{\mathrm{T}}^{\mathrm{miss}}$ events: $\left|\Delta\phi(\{\mathrm{e\ or\ j}\}, \vec{p}_{\mathrm{T}}^{\mathrm{miss}}) - 1.5\right| < E_{\mathrm{T}}^{\mathrm{miss}}/50$ GeV. Events that contain more than one lepton with $p_{\mathrm{T}} > 20$ GeV and $|\eta| < 2.5$ (2.1) for electrons (muons) are rejected.

Events selected for the analysis must contain exactly one electron or muon, at least one small-R

jet near the lepton ($\Delta R(\ell, \text{jet}) < \pi/2$, referred to as the leptonic side), and one large-R jet away from the lepton ($\Delta R(\ell, \text{jet}) > \pi/2$, referred to as the hadronic side). These events are next separated into three exclusive event categories with different signal and background admixtures: "0t", "1t+0b", and "1t+1b". The 0t events are defined by requiring that no hadronic-side jet pass the t tagging selection. For the 1t+0b events, the hadronic-side jet must pass the t tagging selection, and no leptonic-side jets can be b tagged. The third category of 1t+1b events must contain both a hadronic-side t-tagged jet and a leptonic-side b-tagged jet. The 0t sample is dominated by background events, primarily from W+jets production, while the signal and background yields for the 1t+0b sample are expected to be of comparable size. The 1t+1b sample is dominated by signal events.

4   Background estimation

The dominant sources of background are single top quark production (primarily from the Wt channel), W+jets production, and multijet production. In addition, $t\bar{t}$ events with decays to τ+jets (resulting in either hadronic or leptonic final states) or any other than e/μ+jets final states are treated as background in the measurement, and hereafter referred to as "$t\bar{t}$ other". Other sources of background, including diboson, Z+jets, WH, and $t\bar{t}$W/Z production, were found to be negligible. All background normalizations are extracted through a maximum-likelihood fit discussed in Section 6, while the signal and all background distributions are modeled using simulation, except multijet production, which is obtained from data. The $t\bar{t}$ other contribution is constrained to have the same relative normalization as the $t\bar{t}$ signal in the likelihood fit.

The background from multijet production is estimated using control samples in data. Multijet templates for each event category (0t, 1t+0b, 1t+1b) are extracted using control samples, defined by inverting the 2D lepton-jet separation requirement and subtracting residual contributions (corresponding to 3–15% of events in the control samples) from $t\bar{t}$, single top quark, and W+jets events. An initial multijet background normalization is obtained for each event category from a fit of multijet and other signal and background templates to the E_T^{miss} distribution in data.

5   Systematic uncertainties

Systematic uncertainties in the measurement arise from reconstruction and detector resolution effects, background estimation, and theoretical uncertainty in the modeling of signal. The dominant experimental uncertainty is the uncertainty in the t tagging efficiency. The different sources of systematic uncertainty are described in detail below.

The uncertainty in the t tagging efficiency and the corresponding data-to-simulation correction factor are evaluated in Ref. [39]. Since there is a large overlap between those events and events in the signal region in this measurement, and since the t tagging efficiency is strongly anticorrelated with the $t\bar{t}$ cross section measurement, the t tagging efficiency and its uncertainty are determined simultaneously with the cross section (see Section 6.1). The resulting efficiency is in agreement with the previous measurement [39].

The uncertainties in jet energy scale are estimated by changing the jet energy as a function of jet p_T and η by ± 1 standard deviation [31]. These uncertainties, which include differences in jet response between light- and heavy-flavor jets, have been measured for anti-k_T jets with distance parameters of $R = 0.5$ and 0.7, but not for $R = 0.8$ CA jets. The response of the $R = 0.8$ CA jets is estimated in simulation to be within 1% of the response of $R = 0.7$ anti-k_T jets. This is checked by comparing the reconstructed W boson mass in data and simulation in moderately

boosted $t\bar{t}$ events (outside of the signal region). An additional 1% uncertainty is used to account for the small differences observed in these studies. The jet energy scale uncertainties for $R = 0.5$ and $R = 0.8$ jets are treated as fully correlated.

The jet energy resolution is known to be about 10% worse in data than in simulation, and the resolution is therefore adjusted in simulation, using smearing factors in bins of jet η [31]. An associated systematic uncertainty is obtained by rescaling the resolution smearing in simulation by ± 1 standard deviation. This corresponds to changes in the smearing of about $\pm(2.4–5.0)\%$, depending on η. The effect of jet mass scale and jet mass resolution were found to be very small compared to those from the jet energy. These are accounted for with the data-to-simulation correction factor.

The uncertainties associated with the jet energy scale and resolution are propagated to the estimation of the E_T^{miss}. The uncertainty in the modeling of the large-R jet mass, which was measured in Ref. [42], is also accounted for through propagating the jet energy uncertainties to the full jet four-vector.

In addition to uncertainties in the distributions, we also consider several normalization uncertainties affecting the signal yield. The uncertainties in background yields are taken into account in the combined signal-and-background maximum-likelihood fit by changing the W+jets, single top quark, and multijet normalizations, assuming conservative log-normal prior uncertainties of $\pm 50\%$, $\pm 50\%$, and $\pm 100\%$, respectively. The background normalizations are constrained in the maximum-likelihood fit, and corresponding background uncertainties extracted as the ± 1 standard deviation uncertainties in the fit. In addition, the statistical uncertainty resulting from the finite sizes of the simulated samples are included. The uncertainty in the measurement of the integrated luminosity of $\pm 2.6\%$ [16] is also included.

The uncertainty in the pileup modeling is evaluated by varying the total inelastic pp cross section used in the simulation within its uncertainty of $\pm 5\%$ [43]. The resulting uncertainty in the cross section measurements is less than 1%.

Systematic uncertainties from the lepton trigger and corrections to the lepton identification efficiencies that are applied to all simulated events contribute negligibly to the uncertainty in the cross section measurement. This includes the lepton η dependence of these uncertainties. The uncertainty in the b tagging efficiency [35, 36] is also considered, but has a negligible impact on the final result since the measurements are performed by combining events in the 1t+0b and 1t+1b event categories. Uncertainties pertaining to the modeling of the secondary-vertex mass, which is one of the variables used in the maximum-likelihood fit, are negligible compared to the statistical uncertainty in the sample.

Theoretical uncertainties in the modeling of the $t\bar{t}$ events originate from the choice of PDF and renormalization and factorization (μ_R and μ_F) scales, whose nominal values are chosen to be equal to the momentum transfer Q in the hard scattering, given by $Q^2 = m_{\text{top}}^2$, where the summation runs over all final-state partons in the event. The uncertainty in the modeling of the hard-scattering process is evaluated using samples where the renormalization and factorization scales are simultaneously changed up ($2Q$) or down ($Q/2$). The uncertainty from the PDF is evaluated using the up and down eigenvector outputs from the NNLO PDF sets CT10 [29], MSTW 2008 [44], and NNPDF2.3 [45], following the PDF4LHC prescription [46, 47]. An additional theoretical uncertainty is assigned to account for the choice of event generator and parton shower algorithm in extracting the integrated and differential cross sections, evaluated using MC@NLO+HERWIG6 (see Sections 6.1 and 6.3).

6 Cross section measurements

The $t\bar{t}$ signal yield, background normalizations, and t tagging efficiency are extracted simultaneously using a binned, extended maximum-likelihood fit to different templates of several kinematic variables described below. First, the fit is used to determine the integrated $t\bar{t}$ cross section for $p_T^t > 400\,\text{GeV}$, providing a simultaneous measurement of the cross section with nuisance parameters and constraints on the background yields in the data. The results are then used to obtain the differential $t\bar{t}$ cross section as a function of p_T^t and y^t. The cross sections are presented at both the particle and parton levels.

6.1 Maximum-likelihood fit

Three exclusive event categories are used in the maximum-likelihood fit (0t, 1t+0b, 1t+1b), as defined in Section 3. The lepton $|\eta|$ is used as the discriminant for events in the 0t and 1t+0b categories, while m_{vtx} is used to discriminate $t\bar{t}$ events ($t\bar{t}$ signal and $t\bar{t}$ other are constrained to the same relative normalization in the fit) from non-$t\bar{t}$ background in the 1t+1b event category. The electron and muon channels are fitted separately, yielding a total of six categories. The maximum-likelihood fit is performed within the THETA framework [48].

Background normalizations and experimental systematic uncertainties are treated as nuisance parameters in the fit, three of which are built into the model as uncertainties in the input distributions, these being the jet energy scale, jet energy resolution, and t tagging efficiency. The event categories for the fit are designed such that the t tagging efficiency is constrained by the relative populations of events in the different categories. The $t\bar{t}$ cross section and the background normalizations are therefore correlated with these variables. The strongest correlation with the $t\bar{t}$ cross section is the t tagging efficiency. A log-normal prior constraint is used for each nuisance parameter that corresponds to a normalization uncertainty, while uncertainties based on the form of the distributions are modeled with a Gaussian prior for the nuisance parameter, which is used to interpolate between the nominal and shifted templates. The e+jets and μ+jets events use common nuisance parameters for all systematic uncertainties and background normalizations, except for multijet backgrounds, which are taken as independent of each other. The total fitted uncertainties in the background yields are 46% for single top quark, 7.5% for $t\bar{t}$ other, 6.8% for W+jets production, and 47% and 17%, respectively, for the muon and electron multijet backgrounds.

A correction factor to account for small differences in the t tagging efficiency between data and simulation is also determined through the maximum-likelihood fit. While the dependence of this efficiency correction on the t jet η is taken from Ref. [39], an additional uncertainty to account for a potential dependence of p_T^t is evaluated by performing separate fits for events with $p_T^t < 600\,\text{GeV}$ and $>600\,\text{GeV}$. All other nuisance parameters are required to be the same in both p_T^t regions for this check. An additional uncertainty of 17% is assigned for $p_T^t > 600\,\text{GeV}$ to account for the p_T dependence, resulting in a total uncertainty in the t tagging efficiency of $\pm 5\%$ ($\pm 18\%$) for $p_T^t < 600$ (>600) GeV.

The measured normalizations in the signal and background yields, as determined from the maximum-likelihood fit, are given, together with the number of observed events in data, in Table 1. The electron and muon channels are shown separately. The quoted uncertainties are from the total fit, and include the statistical components, but not the theoretical uncertainties in the $t\bar{t}$ signal. The total signal and background yields are consistent with the observed number of events in the data within about one standard deviation.

The distributions in $|\eta|$ and m_{vtx} after the combined maximum-likelihood fit to e+jets and μ+jets

Table 1:   Predicted numbers of signal and background events, as well as the total yield, together with the observed number of events in data, are shown after the combined maximum-likelihood fit for the e+jets (top) and μ+jets (bottom) categories. The uncertainties include the statistical component from the fit, but not the theoretical uncertainties in the tt̄ signal. The uncertainties in the sum of backgrounds and the total yield are determined neglecting correlations for presentational purposes, although the full likelihood with correlations is used to compute the uncertainties in the measurements of the cross section.

Sample	Number of events (e+jets)		
	0t	1t+0b	1t+1b
tt̄ signal	1560 ± 120	289 ± 22	226 ± 17
tt̄ other	458 ± 34	40.0 ± 3.0	30.1 ± 2.3
Single t	260 ± 120	11.6 ± 5.3	3.2 ± 1.5
W+jets	3670 ± 250	130 ± 9	2.7 ± 0.2
Multijet	760 ± 130	68 ± 11	10.5 ± 1.8
Total background	5140 ± 310	249 ± 16	46.5 ± 3.2
Signal + background	6700 ± 330	537 ± 27	273 ± 17
Data	6833	538	242

Sample	Number of events (μ+jets)		
	0t	1t+0b	1t+1b
tt̄ signal	1920 ± 140	359 ± 27	271 ± 20
tt̄ other	478 ± 36	44.7 ± 3.4	29.7 ± 2.2
Single t	290 ± 140	14.4 ± 6.6	4.1 ± 1.9
W+jets	4790 ± 330	154 ± 11	3.9 ± 0.3
Multijet	360 ± 170	13.4 ± 6.3	7.6 ± 3.6
Total background	5920 ± 390	226 ± 14	45.3 ± 4.6
Signal + background	7840 ± 420	586 ± 31	317 ± 21
Data	7712	622	306

events are shown in Fig. 1, comparing the fitted values of the model to the data from each of the fitted categories (0t, 1t+0b, 1t+1b). The uncertainty bands show the combined fitted statistical and experimental systematic uncertainties in the signal and backgrounds, added in quadrature neglecting correlations for presentational purposes, although the full likelihood with correlations is used to compute the uncertainties in the measurements of the cross section. The p_T and y distributions of the hadronic-side, large-R jet are shown for each category in Fig. 2.   These figures show the data, together with the signal and background yields from simulation (or, for multijet background, from data enhanced with multijet events), using the normalizations from the fit, as well as the ratio of the data to the total fit. Since the p_T^t and y^t variables are not used in the fit, the signal and background distributions in Fig. 2 are taken from simulation (or the data sideband for the multijet background). In extracting the differential cross sections, these distributions are used for the backgrounds, while the signal is taken from the data after subtracting the background contributions.

6.2   Integrated tt̄ cross section measurement

The measurement at the particle level is defined within a fiducial region designed to closely match the event selections in the detector and minimize the dependence on theoretical input. The measurement at the parton level is defined relative to the top and antitop quarks before they decay, but after they radiate any gluons.
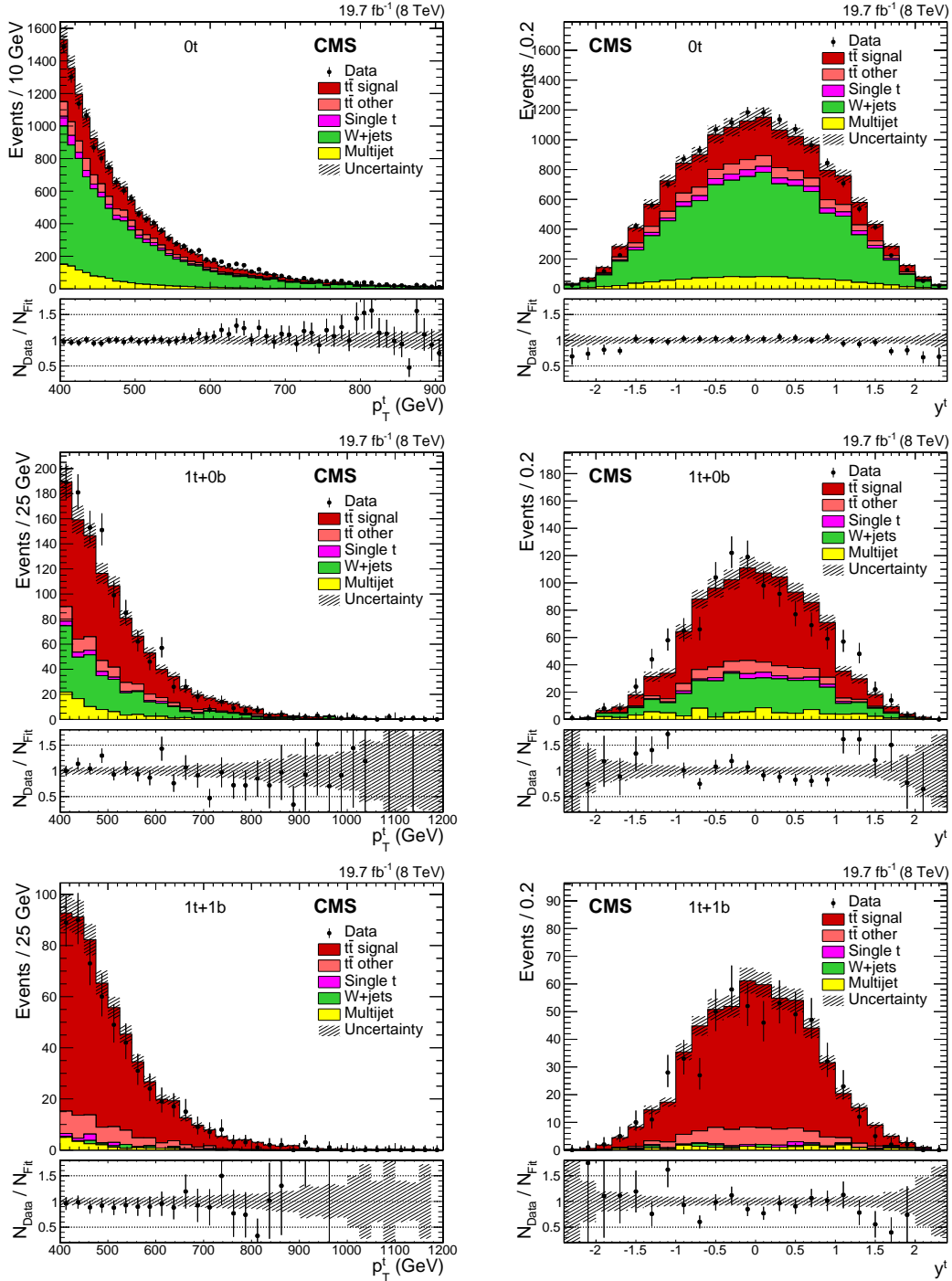
Figure 1: Lepton $|\eta|$ and m_{vtx} distributions from data (points) and for signal and background sources (histograms) with normalizations from the fit for the 0t (top), 1t+0b (middle), and 1t+1b (bottom) event categories, for the e+jets (left column) and μ+jets (right column) channels. The vertical bars on the data points represent the statistical uncertainties. The shaded bands reflect the combined statistical and experimental systematic uncertainties after the fit to the signal and background yields, added in quadrature neglecting their correlations for presentational purposes. The ratios of data (N_{Data}) to the total prediction from the fit (N_{Fit}) are shown below each panel, along with the uncertainty band from the fit.

Figure 2: Transverse momentum (left column) and rapidity (right column) distributions of the hadronic-side, large-R jet for the 0t (top), 1t+0b (middle), and 1t+1b (bottom) event categories, combining the e+jets and μ+jets channels. The data are compared to the total signal and background yields using normalizations from the maximum-likelihood fit. The vertical bars on the data points represent the statistical uncertainties. The shaded bands reflect the combination of the statistical and post-fit systematic uncertainties in the signal and background yields added in quadrature, without the uncertainties based on the form of the distributions, and neglecting their correlations for presentational purposes. The ratios of data (N_{Data}) to the total prediction from the fit (N_{Fit}) are shown below each panel, along with the uncertainty band from the fit.

The POWHEG+PYTHIA6 simulation is used to determine the acceptance for the particle-level and parton-level selections and to obtain the predicted cross section values. The following particle-level selections are used to define the fiducial region in the simulation:

(i) One electron or muon with $p_T > 45\,\text{GeV}$ (computed prior to any potential photon radiation) and $|\eta| < 2.1$.

(ii) At least one anti-k_T ($R = 0.5$) jet with $0.1 < \Delta R(\ell, \text{jet}) < \pi/2$, $p_T > 30\,\text{GeV}$, and $|\eta| < 2.4$.

(iii) At least one CA ($R = 0.8$) jet with $\Delta R(\ell, \text{jet}) > \pi/2$, $p_T > 400\,\text{GeV}$, $140 < m_j < 250\,\text{GeV}$, and $|\eta| < 2.4$.

Jets at the particle level in the simulation are formed from stable particles, excluding electrons, muons, and neutrinos. The cross section at parton level is measured for the region where the top or antitop quark that decays to quarks has $p_T > 400\,\text{GeV}$. No other kinematic requirements are imposed.

The measurements at both the particle and parton levels are corrected for the branching fraction of $t\bar{t} \to e/\mu+\text{jets}$, determined from the $t\bar{t}$ simulation.

The integrated $t\bar{t}$ cross section is obtained from the $t\bar{t}$ signal yield in the maximum-likelihood fit. Uncertainties associated with the signal modeling are not included as nuisance parameters in the fit. These are instead evaluated through the difference in the signal acceptance from changes made in the μ_R and μ_F scales and PDF variations. The uncertainties from the choice of event generator and parton shower algorithm are also evaluated independently of the fit through the difference in the $t\bar{t}$ signal acceptance between the POWHEG+PYTHIA6 and MC@NLO+HERWIG6 predictions at the particle and parton levels.

The measurements of the integrated cross sections for $p_T^t > 400\,\text{GeV}$ are:

$$\text{particle level: } \sigma_{t\bar{t}} = 0.499 \pm 0.035\,\text{(stat+syst)} \pm 0.095\,\text{(theo)} \pm 0.013\,\text{(lumi) pb},$$
$$\text{parton level: } \sigma_{t\bar{t}} = 1.44 \pm 0.10\,\text{(stat+syst)} \pm 0.29\,\text{(theo)} \pm 0.04\,\text{(lumi) pb}.$$

The theoretical uncertainties from the PDF, μ_R and μ_F scales, and choice of event generator and parton shower algorithm are, respectively, 9%, 9%, and 14% at the particle level, and 9%, 10%, and 15% at the parton level.

The measurements are compared to predictions from different $t\bar{t}$ simulations. Assuming the NNLO cross section of 252.9 pb [49] for the full phase space, the resulting POWHEG+PYTHIA6 cross section is 0.580 (1.67) pb at particle (parton) level. The ratio of the measured integrated $t\bar{t}$ cross section for the high-p_T region to the value predicted by the POWHEG+PYTHIA6 simulation is 0.86 ± 0.16 (0.86 ± 0.19) for the particle (parton) level. Thus, the measurements and predictions are consistent within the total uncertainty, which is dominated by the theoretical uncertainty in the cross section extraction. The integrated cross sections are also extracted from the MADGRAPH+PYTHIA6 and MC@NLO+HERWIG6 simulations, again assuming the NNLO cross section for the full phase space, and are 0.675 (1.85) pb and 0.499 (1.42) pb at the particle (parton) level, respectively. The prediction from the MC@NLO+HERWIG6 simulation agrees well with the measured values, while the MADGRAPH+PYTHIA6 simulation overestimates the cross sections at both particle and parton levels.

6.3 Differential $t\bar{t}$ cross section measurements

The differential $t\bar{t}$ cross section is measured as a function of the p_T and y of the top quark that decays to a hadronic final state. The event sample from which the p_T and y distributions of the

t jet candidates are extracted is defined by combining the signal-dominated 1t+0b and 1t+1b event categories. The observed number of t̄t events at detector level is first extracted from data by subtracting the SM background contributions using the normalizations from the maximum-likelihood fit (shown in Table 1). As a cross-check, it is verified that a small t̄t contribution added to the maximum-likelihood fit from a beyond-the-SM process, such as a 1–2% contribution from $Z' \to t\bar{t}$ (corresponding to a signal cross section already excluded in Ref. [13]), has a negligible impact on the extracted SM backgrounds. We also verify that a small potential modification of the top quark rapidity has a minimal impact on the background normalizations that is well within the quoted background normalization uncertainties.

An unfolding procedure translates the observed number of t̄t events in bins of reconstructed p_T and y of the t jet candidate to a cross section in bins of particle- and parton-level top quark p_T^t and y^t. If more than large-R jet fulfills the particle-level selection in Section 6.2, which occurs for <1% of events, the one with highest p_T is chosen as the particle-level t jet. The unfolding accounts for all reconstruction and detector efficiencies, detector resolution effects, and migrations of t̄t events across bins. The unfolding is performed using response matrices, determined with simulated POWHEG+PYTHIA6 t̄t events, using the singular-value-decomposition (SVD) method [50] in the ROOUNFOLD package [51].

The background-subtracted data are unfolded in two steps, first from detector level to particle level, and in a second step from particle level to parton level. Response matrices are created between the p_T and y of the reconstructed t jet candidate and the particle-level t jet, and between the particle-level t jet and the parton-level top quark. These response matrices are used to unfold the data and obtain the differential cross sections, after dividing by the bin width and correcting for the branching fraction of $t\bar{t} \to e/\mu$+jets. The unfolding is performed multiple times, repeating the procedure for each systematic change that affects the p_T^t or y^t distributions. The electron and muon channels are unfolded separately, and are then combined through the statistically weighted mean in each bin. Specifically, the combined cross section in a bin (σ) is given by $\sigma = \sum(\sigma_i/\delta\sigma_i^2) / \sum(1/\delta\sigma_i^2)$, where σ_i is the cross section in a bin for each channel ($i = e, \mu$) and $\delta\sigma_i$ is the corresponding uncertainty. The statistical uncertainty in the combined cross section ($\delta\sigma$) is given by $\delta\sigma = 1/(\sum(1/\delta\sigma_i^2))^{1/2}$. The combination is repeated for each systematic variation, and the difference with respect to the combined nominal value is taken as the uncertainty for that source of systematic bias. The uncertainty in the normalization of the background is extracted by rescaling the subtracted background by ±1 standard deviation, as derived from the maximum-likelihood fit in Section 6.1, and taking the difference in the unfolded result relative to the nominal yield as the uncertainty at particle and parton level, respectively. Similarly, the t tagging efficiency uncertainty as measured at detector level is translated into an uncertainty in the differential measurement at particle and parton levels by unfolding, assuming systematically varied t tagging efficiencies. The uncertainties from the choice of event generator and parton shower algorithm are evaluated by unfolding the nominal POWHEG+PYTHIA6 simulated events using the response matrix from MC@NLO+HERWIG6. The differences between the unfolded simulation and the predictions at the particle and parton levels are taken as the uncertainties. At particle (parton) level, these are 1–18% (2–21%) and 3–8% (2–6%) for the p_T^t and y^t measurements, respectively.

The unfolded results at the particle and parton levels, including all experimental and theoretical uncertainties, are shown as a function of p_T^t and y^t as the data points in Fig. 3, and the relative uncertainties are displayed in Fig. 4. As a consequence of bin migrations, the uncertainties at particle and parton level differ from the corresponding bin-by-bin uncertainties at detector level.
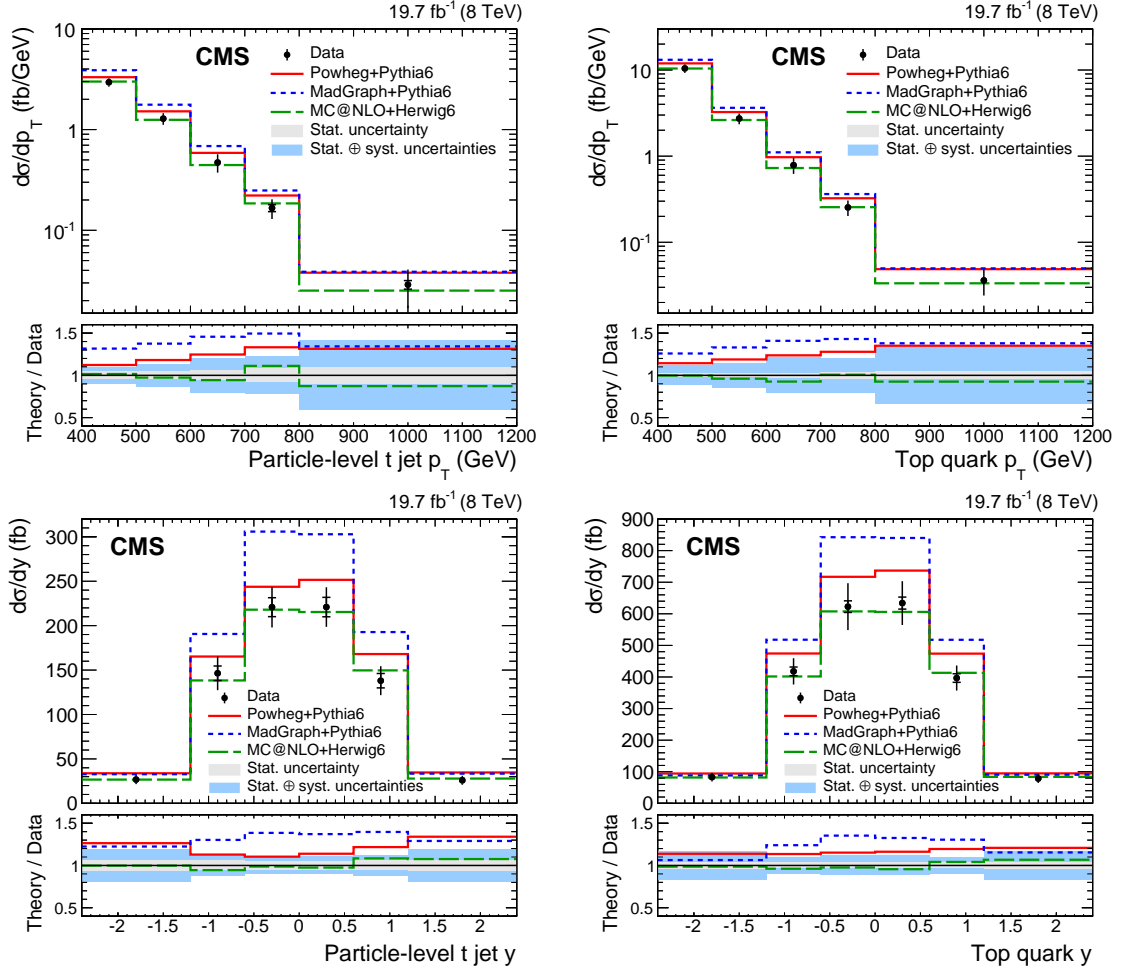
Figure 3: Differential $t\bar{t}$ cross section in bins of particle-level t jet p_T (top left), parton-level top quark p_T (top right), particle-level t jet y (bottom left), and parton-level top quark y (bottom right), including all systematic uncertainties. The lower plots show the ratio of the theoretical predictions to the data. The statistical uncertainties are represented by the inner vertical bars with ticks and the light bands in the ratios. The combined uncertainties are shown as full vertical bars and the dark solid bands in the ratios.
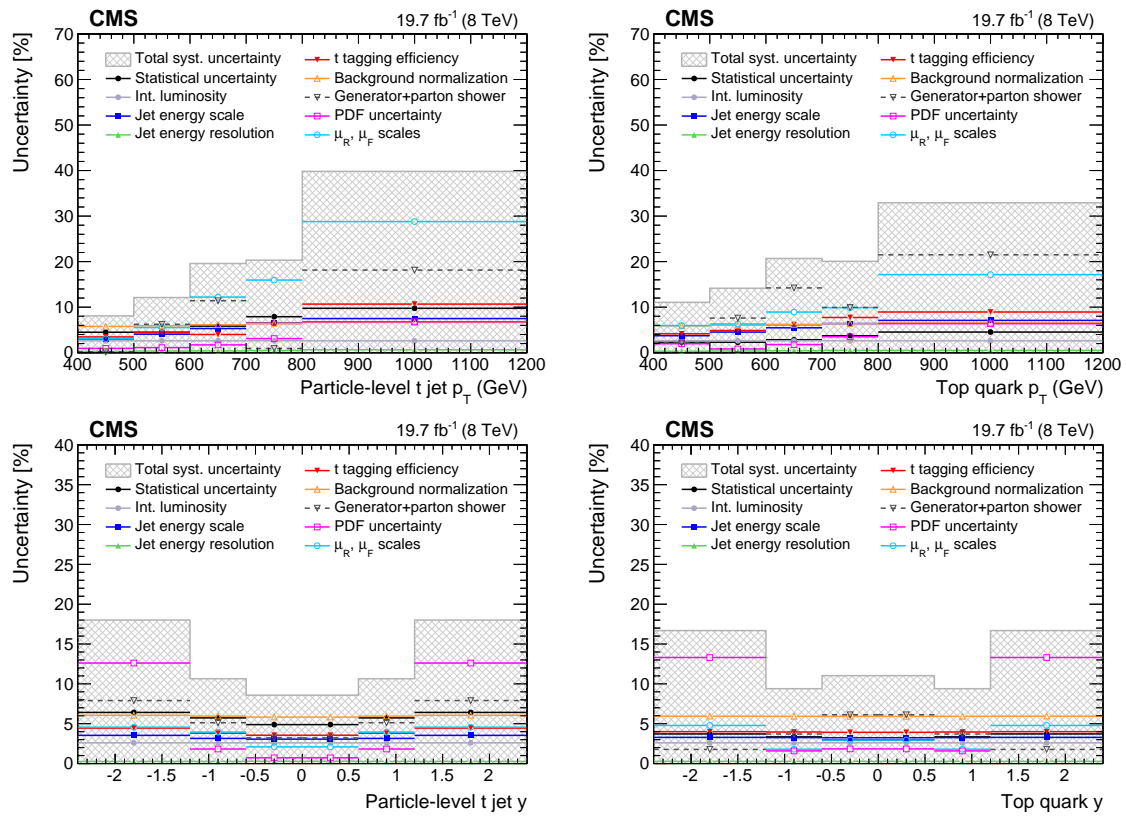
Figure 4: Total systematic uncertainties (cross-hatched regions), as well as individual contributions and statistical-only uncertainties (points) in percent as a function of particle-level t jet p_T (top left), parton-level top quark p_T (top right), particle-level t jet y (bottom left), and parton-level top quark y (bottom right) for the differential cross section measurements. The horizontal bars on the points show the bin widths.

The measured $t\bar{t}$ cross sections are listed in bins of p_T^t and y^t at the particle and parton levels in Table 2. The measured cross sections are compared to the theoretical predictions from the POWHEG+PYTHIA6, MADGRAPH+PYTHIA6, and MC@NLO+HERWIG6 $t\bar{t}$ simulations, all normalized to the NNLO cross section [49]. Their values are also displayed in Fig. 3 and given in Table 2. Also listed in Table 2 are the different relative uncertainties in the measurements, separated into the statistical uncertainty (Stat), the combined experimental uncertainty (Exp), the theoretical uncertainty (Th), and the total measurement uncertainty (Tot), all in percent. The measured cross sections are lower than the predictions from POWHEG+PYTHIA6 and MAD-GRAPH+PYTHIA6, in particular for the high-p_T^t region, while MC@NLO+HERWIG6 gives a better modeling of the data across the full p_T^t range. The differential cross sections are significantly overestimated for $|y^t| < 1.2$ by MADGRAPH+PYTHIA6 as compared to the data. The predictions of the y^t distributions by MC@NLO+HERWIG6 and POWHEG+PYTHIA6 agree with the data within the measurement uncertainties.

Table 2: Differential $t\bar{t}$ cross section in bins of p_T and y for the t jet at the particle level (top) and the top quark at parton level (bottom). The measurements are compared to predictions from the POWHEG+PYTHIA6, MADGRAPH+PYTHIA6, and MC@NLO+HERWIG6 simulations. The total relative uncertainty (Tot) in the measurements is separated into relative statistical (Stat), experimental (Exp), and theoretical (Th) components, all in percent.

p_T (GeV)	$d\sigma/dp_T$ (fb/GeV) at particle level							
	Data	Stat (%)	Exp (%)	Th (%)	Tot (%)	POWHEG	MADGRAPH	MC@NLO
400–500	2.95	4.5	7.4	3.2	9.6	3.32	3.89	3.00
500–600	1.29	4.5	8.4	8.6	13	1.52	1.77	1.25
600–700	0.471	5.8	9.1	17	21	0.587	0.686	0.445
700–800	0.166	7.9	11	16	22	0.222	0.249	0.185
800–1200	0.029	9.7	15	37	41	0.038	0.039	0.025
y	$d\sigma/dy$ (fb) at particle level							
$(-2.4, -1.2)$	27	6.4	8.3	16	19	34	33	27
$(-1.2, -0.6)$	146	5.8	7.8	7.1	12	165	191	138
$(-0.6, 0.0)$	221	4.9	7.5	4.1	10	244	306	218
$(0.0, 0.6)$	221	4.9	7.5	4.1	10	252	303	215
$(0.6, 1.2)$	138	5.8	7.8	7.1	12	168	193	150
$(1.2, 2.4)$	26	6.4	8.3	16	19	35	33	28

p_T (GeV)	$d\sigma/dp_T$ (fb/GeV) at parton level							
	Data	Stat (%)	Exp (%)	Th (%)	Tot (%)	POWHEG	MADGRAPH	MC@NLO
400–500	10.4	2.3	8.1	6.8	11	11.9	13.1	10.4
500–600	2.74	2.3	9.0	10	14	3.25	3.64	2.63
600–700	0.786	2.8	10	18	21	0.972	1.11	0.728
700–800	0.254	3.7	12	16	20	0.324	0.363	0.256
800–1200	0.036	4.5	13	30	33	0.049	0.050	0.033
y	$d\sigma/dy$ (fb) at parton level							
$(-2.4, -1.2)$	83	3.7	7.9	14	17	94	88	82
$(-1.2, -0.6)$	418	3.4	7.8	4.5	10	474	518	402
$(-0.6, 0.0)$	623	3.0	7.8	7.3	11	717	842	608
$(0.0, 0.6)$	634	3.0	7.8	7.3	11	737	840	606
$(0.6, 1.2)$	397	3.4	7.8	4.5	10	474	518	413
$(1.2, 2.4)$	79	3.7	7.9	14	17	95	91	84

The differential $t\bar{t}$ cross section measurement in bins of parton-level top quark p_T is compared to different theoretical cross section calculations in Fig. 5. Calculations of NNLO differential cross

sections are extracted from Ref. [52] for three different PDF sets (NNPDF3.0 [53], CT14 [54], and MMHT2014 [55]). Approximate next-to-next-to-next-to-leading-order (aNNNLO) predictions corresponding to the results presented in Ref. [56] were provided by the author. The NNLO calculations are in good agreement with the measurement across the full top quark p_T range studied. Predictions for different PDF sets cannot be distinguished given the current measurement uncertainty but are all observed to be consistent with the data. The aNNNLO calculation significantly overestimates the cross section, with an increasing disagreement with higher top quark p_T. An additional check of the unfolding procedure is performed to confirm that the unfolding itself would support such a different p_T spectrum. The POWHEG+PYTHIA6 simulation is unfolded using response matrices derived from the same sample, but reweighting the distribution at detector level by a factor that corresponds to that required to match the aNNNLO prediction at parton level. The scaled and then unfolded simulation reproduces the aNNNLO prediction within the measurement uncertainty.
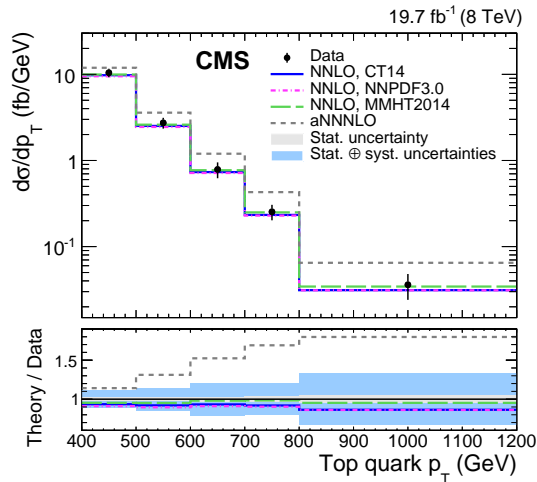
Figure 5: Differential $t\bar{t}$ cross section in bins of parton-level top quark p_T including all systematic uncertainties. The measured cross section is compared to theoretical calculations at NNLO for three different PDF sets [52] and at aNNNLO [56]. The lower plot shows the ratio of these theoretical predictions to the data. The statistical uncertainties are represented by the inner vertical bars with ticks and the light bands in the ratios. The combined uncertainties are shown as full vertical bars and the dark solid bands in the ratios.

7 Summary

The first CMS measurement of the $t\bar{t}$ production cross section in the boosted regime has been presented. The integrated cross section, as well as differential cross sections as a function of the top quark p_T and y, have been measured for $p_T^t > 400\,\text{GeV}$. The measurements use lepton+jets events, identified through an electron or a muon, a b jet candidate from the semileptonic top quark decay, and a t jet candidate from the top quark decaying to a hadronic final state. Backgrounds are modeled using simulations for the distributions, or a data sideband for multijet production. Background normalizations are extracted jointly with the signal yield and the t tagging efficiency using a maximum-likelihood fit.

The integrated cross section measured for $p_T^t > 400\,\text{GeV}$ is $\sigma_{t\bar{t}} = 0.499 \pm 0.035\,(\text{stat+syst}) \pm 0.095\,(\text{theo}) \pm 0.013\,(\text{lumi})\,\text{pb}$ at particle level, and $\sigma_{t\bar{t}} = 1.44 \pm 0.10\,(\text{stat+syst}) \pm 0.29\,(\text{theo}) \pm 0.04\,(\text{lumi})\,\text{pb}$ at parton level, both corrected for the branching fraction of $t\bar{t} \rightarrow e/\mu$+jets. The measurements are compared to the predicted cross section for this p_T range from the

POWHEG+PYTHIA6 $t\bar{t}$ simulation assuming $\sigma_{\text{tot}} = 252.9\,\text{pb}$, which provides a value of $0.580\,\text{pb}$ at particle level and $1.67\,\text{pb}$ at parton level. The cross section for this high-p_T region is therefore found to be overestimated by 14% in the POWHEG+PYTHIA6 simulation, but is consistent within the uncertainties.

Differential cross sections are also measured at both particle and parton levels. Background contributions are subtracted from the t-tagged jet distributions to obtain the distribution for signal. This is unfolded first to the particle level to correct for signal efficiency, acceptance, and bin migrations to yield the cross section in bins of t jet p_T and y at particle level. The data are further unfolded to the parton level to extract the cross section in bins of top quark p_T and y. The measurements are compared to predictions from different $t\bar{t}$ simulations. The POWHEG+PYTHIA6 and MADGRAPH+PYTHIA6 simulations are observed to overestimate the cross section, in particular at high p_T^t, while MC@NLO+HERWIG6 results in a good modeling of the p_T^t spectrum. The POWHEG+PYTHIA6 and MC@NLO+HERWIG6 simulations model the y^t distributions well, while MADGRAPH+PYTHIA6 significantly overestimates the cross section for $|y^t| < 1.2$. The results are compatible with those from the nonboosted CMS measurement [4] in the p_T range where the two analyses overlap (400–500 GeV). The nonboosted measurement also observes an overestimate of the cross section for different MC generators in this p_T range, most prominent for MADGRAPH+PYTHIA6, and an improved modeling of the p_T spectrum using HERWIG 6 for the parton showering. The measurement as a function of parton-level top quark p_T is also compared to theoretical aNNNLO and NNLO calculations. While the aNNNLO prediction significantly overestimate the measurement, especially for high top quark p_T, the NNLO calculations are in good agreement across the full p_T range studied.

The analysis presented in this paper extends the differential $t\bar{t}$ cross section measurement into the $p_T > 1\,\text{TeV}$ range. These measurements will help improve the modeling of event generators in this high-p_T range, an important regime for many new physics searches.

Acknowledgements

References

[1] CMS Collaboration, "The CMS experiment at the CERN LHC", *JINST* **3** (2008) S08004, `doi:10.1088/1748-0221/3/08/S08004`.

[2] ATLAS Collaboration, "The ATLAS experiment at the CERN Large Hadron Collider", *JINST* **3** (2008) S08003, `doi:10.1088/1748-0221/3/08/S08003`.

[3] CMS Collaboration, "Measurement of differential top-quark pair production cross sections in pp colisions at $\sqrt{s} = 7$ TeV", *Eur. Phys. J. C* **73** (2013) 2339, `doi:10.1140/epjc/s10052-013-2339-4`, `arXiv:1211.2220`.

[4] CMS Collaboration, "Measurement of the differential cross section for top quark pair production in pp collisions at $\sqrt{s} = 8$ TeV", *Eur. Phys. J. C* **75** (2015) 542, `doi:10.1140/epjc/s10052-015-3709-x`, `arXiv:1505.04480`.

[5] CMS Collaboration, "Measurement of the $t\bar{t}$ production cross section in the all-jets final state in pp collisions at $\sqrt{s} = 8$ TeV", *Eur. Phys. J. C* **76** (2016) 128, `doi:10.1140/epjc/s10052-016-3956-5`, `arXiv:1509.06076`.

[6] ATLAS Collaboration, "Measurements of top quark pair relative differential cross-sections with ATLAS in pp collisions at $\sqrt{s} = 7$ TeV", *Eur. Phys. J. C* **73** (2013) 2261, `doi:10.1140/epjc/s10052-012-2261-1`, `arXiv:1207.5644`.

[7] ATLAS Collaboration, "Measurements of normalized differential cross sections for $t\bar{t}$ production in pp collisions at $\sqrt{s} = 7$ TeV using the ATLAS detector", *Phys. Rev. D* **90** (2014) 072004, `doi:10.1103/PhysRevD.90.072004`, `arXiv:1407.0371`.

[8] ATLAS Collaboration, "Differential top-antitop cross-section measurements as a function of observables constructed from final-state particles using pp collisions at $\sqrt{s} = 7$ TeV in the ATLAS detector", *JHEP* **06** (2015) 100, `doi:10.1007/JHEP06(2015)100`, `arXiv:1502.05923`.

[9] ATLAS Collaboration, "Measurements of top-quark pair differential cross-sections in the lepton+jets channel in pp collisions at $\sqrt{s} = 8$ TeV using the ATLAS detector", (2015). `arXiv:1511.04716`. Submitted to EPJC.

[10] R. Frederix and F. Maltoni, "Top pair invariant mass distribution: a window on new physics", *JHEP* **01** (2009) 047, `doi:10.1088/1126-6708/2009/01/047`, `arXiv:0712.2355`.

[11] ATLAS Collaboration, "Measurement of the differential cross-section of highly boosted top quarks as a function of their transverse momentum in $\sqrt{s} = 8$ TeV proton-proton collisions using the ATLAS detector", *Phys. Rev. D* **93** (2016) 032009, `doi:10.1103/PhysRevD.93.032009`, `arXiv:1510.03818`.

[12] CMS Collaboration, "Searches for new physics using the $t\bar{t}$ invariant mass distribution in pp collisions at $\sqrt{s} = 8$ TeV", *Phys. Rev. Lett.* **111** (2013) 211804, `doi:10.1103/PhysRevLett.111.211804`, `arXiv:1309.2030`. [Erratum: `doi:10.1103/PhysRevLett.112.119903`].

[13] CMS Collaboration, "Search for resonant $t\bar{t}$ production in proton-proton collisions at $\sqrt{s} = 8$ TeV", *Phys. Rev. D* **93** (2016) 012001, `doi:10.1103/PhysRevD.93.012001`, `arXiv:1506.03062`.

[14] CMS Collaboration, "Particle-flow event reconstruction in CMS and performance for jets, taus, and E_T^{miss}", CMS Physics Analysis Summary CMS-PAS-PFT-09-001, 2009.

[15] CMS Collaboration, "Commissioning of the particle-flow event reconstruction with the first LHC collisions recorded in the CMS detector", CMS Physics Analysis Summary CMS-PAS-PFT-10-001, 2010.

[16] CMS Collaboration, "CMS luminosity based on pixel cluster counting – summer 2013 update", CMS Physics Analysis Summary CMS-PAS-LUM-13-001, 2013.

[17] P. Nason, "A new method for combining NLO QCD with shower Monte Carlo algorithms", *JHEP* **11** (2004) 040, `doi:10.1088/1126-6708/2004/11/040`, `arXiv:hep-ph/0409146`.

[18] S. Frixione, P. Nason, and C. Oleari, "Matching NLO QCD computations with Parton Shower simulations: the POWHEG method", *JHEP* **11** (2007) 070, `doi:10.1088/1126-6708/2007/11/070`, `arXiv:0709.2092`.

[19] S. Alioli, P. Nason, C. Oleari, and E. Re, "A general framework for implementing NLO calculations in shower Monte Carlo programs: the POWHEG BOX", *JHEP* **06** (2010) 043, `doi:10.1007/JHEP06(2010)043`, `arXiv:1002.2581`.

[20] J. M. Campbell, R. K. Ellis, P. Nason, and E. Re, "Top-pair production and decay at NLO matched with parton showers", *JHEP* **04** (2015) 114, `doi:10.1007/JHEP04(2015)114`, `arXiv:1412.1828`.

[21] S. Alioli, P. Nason, C. Oleari, and E. Re, "NLO single-top production matched with shower in POWHEG: *s*- and *t*-channel contributions", *JHEP* **09** (2009) 111, `doi:10.1088/1126-6708/2009/09/111`, `arXiv:0907.4076`. [Erratum: `doi:10.1007/JHEP02(2010)011`].

[22] J. Alwall et al., "The automated computation of tree-level and next-to-leading order differential cross sections, and their matching to parton shower simulations", *JHEP* **07** (2014) 079, `doi:10.1007/JHEP07(2014)079`, `arXiv:1405.0301`.

[23] S. Frixione and B. R. Webber, "Matching NLO QCD computations and parton shower simulations", *JHEP* **06** (2002) 029, `doi:10.1088/1126-6708/2002/06/029`, `arXiv:hep-ph/0204244`.

[24] G. Corcella et al., "HERWIG 6: An Event generator for hadron emission reactions with interfering gluons (including supersymmetric processes)", *JHEP* **01** (2001) 010, `doi:10.1088/1126-6708/2001/01/010`, `arXiv:hep-ph/0011363`.

[25] T. Sjöstrand, S. Mrenna, and P. Skands, "PYTHIA 6.4 physics and manual", *JHEP* **05** (2006) 026, `doi:10.1088/1126-6708/2006/05/026`, `arXiv:hep-ph/0603175`.

[26] M. L. Mangano, M. Moretti, F. Piccinini, and M. Treccani, "Matching matrix elements and shower evolution for top-quark production in hadronic collisions", *JHEP* **01** (2007) 013, `doi:10.1088/1126-6708/2007/01/013`, `arXiv:hep-ph/0611129`.

[27] R. Field, "Early LHC underlying event data – findings and surprises", in *Hadron collider physics. Proceedings, 22nd Conference, HCP 2010, Toronto, Canada, August 23-27, 2010*. 2010. `arXiv:1010.3558`.

[28] J. Pumplin et al., "New generation of parton distributions with uncertainties from global QCD analysis", *JHEP* **07** (2002) 012, `doi:10.1088/1126-6708/2002/07/012`, `arXiv:hep-ph/0201195`.

[29] J. Gao et al., "CT10 next-to-next-to-leading order global analysis of QCD", *Phys. Rev. D* **89** (2014) 033009, `doi:10.1103/PhysRevD.89.033009`, `arXiv:1302.6246`.

[30] GEANT4 Collaboration, "GEANT4—a simulation toolkit", *Nucl. Instrum. Meth. A* **506** (2003) 250, `doi:10.1016/S0168-9002(03)01368-8`.

[31] CMS Collaboration, "Determination of jet energy calibration and transverse momentum resolution in CMS", *JINST* **6** (2011) P11002, `doi:10.1088/1748-0221/6/11/P11002`, `arXiv:1107.4277`.

[32] M. Cacciari, G. P. Salam, and G. Soyez, "The catchment area of jets", *JHEP* **04** (2008) 005, `doi:10.1088/1126-6708/2008/04/005`, `arXiv:0802.1188`.

[33] M. Cacciari, G. P. Salam, and G. Soyez, "FastJet user manual", *Eur. Phys. J. C* **72** (2012) 1896, `doi:10.1140/epjc/s10052-012-1896-2`, `arXiv:1111.6097`.

[34] M. Cacciari, G. P. Salam, and G. Soyez, "The anti-k_t jet clustering algorithm", *JHEP* **04** (2008) 063, `doi:10.1088/1126-6708/2008/04/063`, `arXiv:0802.1189`.

[35] CMS Collaboration, "Identification of b-quark jets with the CMS experiment", *JINST* **8** (2013) P04013, `doi:10.1088/1748-0221/8/04/P04013`, `arXiv:1211.4462`.

[36] CMS Collaboration, "Performance of b-tagging at $\sqrt{s} = 8$ TeV in multijet, $t\bar{t}$ and boosted topology events", CMS Physics Analysis Summary CMS-PAS-BTV-13-001, 2013.

[37] M. Wobisch and T. Wengler, "Hadronization corrections to jet cross sections in deep-inelastic scattering", (1998). `arXiv:hep-ph/9907280`.

[38] Y. L. Dokshitzer, G. D. Leder, S. Moretti, and B. R. Webber, "Better jet clustering algorithms", *JHEP* **08** (1997) 001, `doi:10.1088/1126-6708/1997/08/001`, `arXiv:hep-ph/9707323`.

[39] CMS Collaboration, "Boosted top jet tagging at CMS", CMS Physics Analysis Summary CMS-PAS-JME-13-007, 2014.

[40] CMS Collaboration, "Performance of electron reconstruction and selection with the CMS detector in proton-proton collisions at $\sqrt{s} = 8$ TeV", *JINST* **10** (2015) P06005, `doi:10.1088/1748-0221/10/06/P06005`, `arXiv:1502.02701`.

[41] CMS Collaboration, "Performance of CMS muon reconstruction in pp collision events at $\sqrt{s} = 7$ TeV", *JINST* **7** (2012) P10002, `doi:10.1088/1748-0221/7/10/P10002`, `arXiv:1206.4071`.

[42] CMS Collaboration, "Studies of jet mass in dijet and W/Z + jet events", *JHEP* **05** (2013) 090, `doi:10.1007/JHEP05(2013)090`, `arXiv:1303.4811`.

[43] CMS Collaboration, "Measurement of the inelastic proton-proton cross section at $\sqrt{s} = 7$ TeV", *Phys. Lett. B* **722** (2013) 5, `doi:10.1016/j.physletb.2013.03.024`, `arXiv:1210.6718`.

[44] A. D. Martin, W. J. Stirling, R. S. Thorne, and G. Watt, "Parton distributions for the LHC", *Eur. Phys. J. C* **63** (2009) 189, `doi:10.1140/epjc/s10052-009-1072-5`, `arXiv:0901.0002`.

[45] R. D. Ball et al., "Parton distributions with LHC data", *Nucl. Phys. B* **867** (2013) 244, `doi:10.1016/j.nuclphysb.2012.10.003`, `arXiv:1207.1303`.

[46] S. Alekhin et al., "The PDF4LHC Working Group interim report", (2011). `arXiv:1101.0536`.

[47] M. Botje et al., "The PDF4LHC Working Group interim recommendations", (2011). `arXiv:1101.0538`.

[48] J. Ott, "The Theta package",. `http://www.theta-framework.org/`.

[49] M. Czakon and A. Mitov, "Top++: a program for the calculation of the top-pair cross-section at hadron colliders", *Comput. Phys. Commun.* **185** (2014) 2930, `doi:10.1016/j.cpc.2014.06.021`, `arXiv:1112.5675`.

[50] A. Höcker and V. Kartvelishvili, "SVD approach to data unfolding", *Nucl. Instrum. Meth. A* **372** (1996) 469, `doi:10.1016/0168-9002(95)01478-0`, `arXiv:hep-ph/9509307`.

[51] T. Adye, "Unfolding algorithms and tests using RooUnfold", in *PHYSTAT 2011 Workshop on Statistical Issues Related to Discovery Claims in Search Experiments and Unfolding*, H. Prosper and L. Lyons, eds., p. 313. Geneva, Switzerland, 2011. `arXiv:1105.1160`. `doi:10.5170/CERN-2011-006.313`.

[52] M. Czakon, D. Heymes, and A. Mitov, "Dynamical scales for multi-TeV top-pair production at the LHC", (2016). `arXiv:1606.03350`.

[53] NNPDF Collaboration, "Parton distributions for the LHC Run II", *JHEP* **04** (2015) 040, `doi:10.1007/JHEP04(2015)040`, `arXiv:1410.8849`.

[54] S. Dulat et al., "New parton distribution functions from a global analysis of quantum chromodynamics", *Phys. Rev. D* **93** (2016) 033006, `doi:10.1103/PhysRevD.93.033006`, `arXiv:1506.07443`.

[55] L. A. Harland-Lang, A. D. Martin, P. Motylinski, and R. S. Thorne, "Parton distributions in the LHC era: MMHT 2014 PDFs", *Eur. Phys. J. C* **75** (2015) 204, `doi:10.1140/epjc/s10052-015-3397-6`, `arXiv:1412.3989`.

[56] N. Kidonakis, "NNNLO soft-gluon corrections for the top-quark p_T and rapidity distributions", *Phys. Rev. D* **91** (2015) 031501, `doi:10.1103/PhysRevD.91.031501`, `arXiv:1411.2633`.

A The CMS Collaboration

Yerevan Physics Institute, Yerevan, Armenia
V. Khachatryan, A.M. Sirunyan, A. Tumasyan

Institut für Hochenergiephysik der OeAW, Wien, Austria
W. Adam, E. Asilar, T. Bergauer, J. Brandstetter, E. Brondolin, M. Dragicevic, J. Erö, M. Flechl,
M. Friedl, R. Frühwirth[1], V.M. Ghete, C. Hartl, N. Hörmann, J. Hrubec, M. Jeitler[1], A. König,
M. Krammer[1], I. Krätschmer, D. Liko, T. Matsushita, I. Mikulec, D. Rabady, N. Rad,
B. Rahbaran, H. Rohringer, J. Schieck[1], J. Strauss, W. Treberer-Treberspurg, W. Waltenberger,
C.-E. Wulz[1]

National Centre for Particle and High Energy Physics, Minsk, Belarus
V. Mossolov, N. Shumeiko, J. Suarez Gonzalez

Universiteit Antwerpen, Antwerpen, Belgium
S. Alderweireldt, T. Cornelis, E.A. De Wolf, X. Janssen, A. Knutsson, J. Lauwers, S. Luyckx,
M. Van De Klundert, H. Van Haevermaet, P. Van Mechelen, N. Van Remortel, A. Van Spilbeeck

Vrije Universiteit Brussel, Brussel, Belgium
S. Abu Zeid, F. Blekman, J. D'Hondt, N. Daci, I. De Bruyn, K. Deroover, N. Heracleous,
J. Keaveney, S. Lowette, S. Moortgat, L. Moreels, A. Olbrechts, Q. Python, D. Strom,
S. Tavernier, W. Van Doninck, P. Van Mulders, I. Van Parijs

Université Libre de Bruxelles, Bruxelles, Belgium
H. Brun, C. Caillol, B. Clerbaux, G. De Lentdecker, G. Fasanella, L. Favart, R. Goldouzian,
A. Grebenyuk, G. Karapostoli, T. Lenzi, A. Léonard, T. Maerschalk, A. Marinov, A. Randle-
conde, T. Seva, C. Vander Velde, P. Vanlaer, R. Yonamine, F. Zenoni, F. Zhang[2]

Ghent University, Ghent, Belgium
L. Benucci, A. Cimmino, S. Crucy, D. Dobur, A. Fagot, G. Garcia, M. Gul, J. Mccartin,
A.A. Ocampo Rios, D. Poyraz, D. Ryckbosch, S. Salva, R. Schöfbeck, M. Sigamani, M. Tytgat,
W. Van Driessche, E. Yazgan, N. Zaganidis

Université Catholique de Louvain, Louvain-la-Neuve, Belgium
C. Beluffi[3], O. Bondu, S. Brochet, G. Bruno, A. Caudron, L. Ceard, S. De Visscher, C. Delaere,
M. Delcourt, D. Favart, L. Forthomme, A. Giammanco, A. Jafari, P. Jez, M. Komm, V. Lemaitre,
A. Mertens, M. Musich, C. Nuttens, K. Piotrzkowski, L. Quertenmont, M. Selvaggi, M. Vidal
Marono

Université de Mons, Mons, Belgium
N. Beliy, G.H. Hammad

Centro Brasileiro de Pesquisas Fisicas, Rio de Janeiro, Brazil
W.L. Aldá Júnior, F.L. Alves, G.A. Alves, L. Brito, M. Correa Martins Junior, M. Hamer,
C. Hensel, A. Moraes, M.E. Pol, P. Rebello Teles

Universidade do Estado do Rio de Janeiro, Rio de Janeiro, Brazil
E. Belchior Batista Das Chagas, W. Carvalho, J. Chinellato[4], A. Custódio, E.M. Da Costa,
D. De Jesus Damiao, C. De Oliveira Martins, S. Fonseca De Souza, L.M. Huertas Guativa,
H. Malbouisson, D. Matos Figueiredo, C. Mora Herrera, L. Mundim, H. Nogima, W.L. Prado
Da Silva, A. Santoro, A. Sznajder, E.J. Tonelli Manganote[4], A. Vilela Pereira

Universidade Estadual Paulista [a], Universidade Federal do ABC [b], São Paulo, Brazil
S. Ahuja[a], C.A. Bernardes[b], A. De Souza Santos[b], S. Dogra[a], T.R. Fernandez Perez Tomei[a],

E.M. Gregores[b], P.G. Mercadante[b], C.S. Moon[a,5], S.F. Novaes[a], Sandra S. Padula[a], D. Romero Abad[b], J.C. Ruiz Vargas

Institute for Nuclear Research and Nuclear Energy, Sofia, Bulgaria
A. Aleksandrov, R. Hadjiiska, P. Iaydjiev, M. Rodozov, S. Stoykova, G. Sultanov, M. Vutova

University of Sofia, Sofia, Bulgaria
A. Dimitrov, I. Glushkov, L. Litov, B. Pavlov, P. Petkov

Beihang University, Beijing, China
W. Fang[6]

Institute of High Energy Physics, Beijing, China
M. Ahmad, J.G. Bian, G.M. Chen, H.S. Chen, M. Chen, T. Cheng, R. Du, C.H. Jiang, D. Leggat, R. Plestina[7], F. Romeo, S.M. Shaheen, A. Spiezia, J. Tao, C. Wang, Z. Wang, H. Zhang

State Key Laboratory of Nuclear Physics and Technology, Peking University, Beijing, China
C. Asawatangtrakuldee, Y. Ban, Q. Li, S. Liu, Y. Mao, S.J. Qian, D. Wang, Z. Xu

Universidad de Los Andes, Bogota, Colombia
C. Avila, A. Cabrera, L.F. Chaparro Sierra, C. Florez, J.P. Gomez, B. Gomez Moreno, J.C. Sanabria

University of Split, Faculty of Electrical Engineering, Mechanical Engineering and Naval Architecture, Split, Croatia
N. Godinovic, D. Lelas, I. Puljak, P.M. Ribeiro Cipriano

University of Split, Faculty of Science, Split, Croatia
Z. Antunovic, M. Kovac

Institute Rudjer Boskovic, Zagreb, Croatia
V. Brigljevic, D. Ferencek, K. Kadija, J. Luetic, S. Micanovic, L. Sudic

University of Cyprus, Nicosia, Cyprus
A. Attikis, G. Mavromanolakis, J. Mousa, C. Nicolaou, F. Ptochos, P.A. Razis, H. Rykaczewski

Charles University, Prague, Czech Republic
M. Finger[8], M. Finger Jr.[8]

Universidad San Francisco de Quito, Quito, Ecuador
E. Carrera Jarrin

Academy of Scientific Research and Technology of the Arab Republic of Egypt, Egyptian Network of High Energy Physics, Cairo, Egypt
Y. Assran[9,10], A. Ellithi Kamel[11,11], A. Mahrous[12], A. Radi[10,13]

National Institute of Chemical Physics and Biophysics, Tallinn, Estonia
B. Calpas, M. Kadastik, M. Murumaa, L. Perrini, M. Raidal, A. Tiko, C. Veelken

Department of Physics, University of Helsinki, Helsinki, Finland
P. Eerola, J. Pekkanen, M. Voutilainen

Helsinki Institute of Physics, Helsinki, Finland
J. Härkönen, V. Karimäki, R. Kinnunen, T. Lampén, K. Lassila-Perini, S. Lehti, T. Lindén, P. Luukka, T. Peltola, J. Tuominiemi, E. Tuovinen, L. Wendland

Lappeenranta University of Technology, Lappeenranta, Finland
J. Talvitie, T. Tuuva

DSM/IRFU, CEA/Saclay, Gif-sur-Yvette, France
M. Besancon, F. Couderc, M. Dejardin, D. Denegri, B. Fabbro, J.L. Faure, C. Favaro, F. Ferri, S. Ganjour, A. Givernaud, P. Gras, G. Hamel de Monchenault, P. Jarry, E. Locci, M. Machet, J. Malcles, J. Rander, A. Rosowsky, M. Titov, A. Zghiche

Laboratoire Leprince-Ringuet, Ecole Polytechnique, IN2P3-CNRS, Palaiseau, France
A. Abdulsalam, I. Antropov, S. Baffioni, F. Beaudette, P. Busson, L. Cadamuro, E. Chapon, C. Charlot, O. Davignon, L. Dobrzynski, R. Granier de Cassagnac, M. Jo, S. Lisniak, P. Miné, I.N. Naranjo, M. Nguyen, C. Ochando, G. Ortona, P. Paganini, P. Pigard, S. Regnard, R. Salerno, Y. Sirois, T. Strebler, Y. Yilmaz, A. Zabi

Institut Pluridisciplinaire Hubert Curien, Université de Strasbourg, Université de Haute Alsace Mulhouse, CNRS/IN2P3, Strasbourg, France
J.-L. Agram[14], J. Andrea, A. Aubin, D. Bloch, J.-M. Brom, M. Buttignol, E.C. Chabert, N. Chanon, C. Collard, E. Conte[14], X. Coubez, J.-C. Fontaine[14], D. Gelé, U. Goerlach, C. Goetzmann, A.-C. Le Bihan, J.A. Merlin[15], K. Skovpen, P. Van Hove

Centre de Calcul de l'Institut National de Physique Nucleaire et de Physique des Particules, CNRS/IN2P3, Villeurbanne, France
S. Gadrat

Université de Lyon, Université Claude Bernard Lyon 1, CNRS-IN2P3, Institut de Physique Nucléaire de Lyon, Villeurbanne, France
S. Beauceron, C. Bernet, G. Boudoul, E. Bouvier, C.A. Carrillo Montoya, R. Chierici, D. Contardo, B. Courbon, P. Depasse, H. El Mamouni, J. Fan, J. Fay, S. Gascon, M. Gouzevitch, B. Ille, F. Lagarde, I.B. Laktineh, M. Lethuillier, L. Mirabito, A.L. Pequegnot, S. Perries, A. Popov[16], J.D. Ruiz Alvarez, D. Sabes, V. Sordini, M. Vander Donckt, P. Verdier, S. Viret

Georgian Technical University, Tbilisi, Georgia
T. Toriashvili[17]

Tbilisi State University, Tbilisi, Georgia
Z. Tsamalaidze[8]

RWTH Aachen University, I. Physikalisches Institut, Aachen, Germany
C. Autermann, S. Beranek, L. Feld, A. Heister, M.K. Kiesel, K. Klein, M. Lipinski, A. Ostapchuk, M. Preuten, F. Raupach, S. Schael, C. Schomakers, J.F. Schulte, J. Schulz, T. Verlage, H. Weber, V. Zhukov[16]

RWTH Aachen University, III. Physikalisches Institut A, Aachen, Germany
M. Ata, M. Brodski, E. Dietz-Laursonn, D. Duchardt, M. Endres, M. Erdmann, S. Erdweg, T. Esch, R. Fischer, A. Güth, T. Hebbeker, C. Heidemann, K. Hoepfner, S. Knutzen, M. Merschmeyer, A. Meyer, P. Millet, S. Mukherjee, M. Olschewski, K. Padeken, P. Papacz, T. Pook, M. Radziej, H. Reithler, M. Rieger, F. Scheuch, L. Sonnenschein, D. Teyssier, S. Thüer

RWTH Aachen University, III. Physikalisches Institut B, Aachen, Germany
V. Cherepanov, Y. Erdogan, G. Flügge, H. Geenen, M. Geisler, F. Hoehle, B. Kargoll, T. Kress, A. Künsken, J. Lingemann, A. Nehrkorn, A. Nowack, I.M. Nugent, C. Pistone, O. Pooth, A. Stahl[15]

Deutsches Elektronen-Synchrotron, Hamburg, Germany
M. Aldaya Martin, I. Asin, K. Beernaert, O. Behnke, U. Behrens, K. Borras[18], A. Campbell, P. Connor, C. Contreras-Campana, F. Costanza, C. Diez Pardos, G. Dolinska, S. Dooling, G. Eckerlin, D. Eckstein, T. Eichhorn, E. Gallo[19], J. Garay Garcia, A. Geiser, A. Gizhko,

J.M. Grados Luyando, P. Gunnellini, A. Harb, J. Hauk, M. Hempel[20], H. Jung, A. Kalogeropoulos, O. Karacheban[20], M. Kasemann, J. Kieseler, C. Kleinwort, I. Korol, W. Lange, A. Lelek, J. Leonard, K. Lipka, A. Lobanov, W. Lohmann[20], R. Mankel, I.-A. Melzer-Pellmann, A.B. Meyer, G. Mittag, J. Mnich, A. Mussgiller, E. Ntomari, D. Pitzl, R. Placakyte, A. Raspereza, B. Roland, M.Ö. Sahin, P. Saxena, T. Schoerner-Sadenius, C. Seitz, S. Spannagel, N. Stefaniuk, K.D. Trippkewitz, G.P. Van Onsem, R. Walsh, C. Wissing

University of Hamburg, Hamburg, Germany
V. Blobel, M. Centis Vignali, A.R. Draeger, T. Dreyer, J. Erfle, E. Garutti, K. Goebel, D. Gonzalez, M. Görner, J. Haller, M. Hoffmann, R.S. Höing, A. Junkes, R. Klanner, R. Kogler, N. Kovalchuk, T. Lapsien, T. Lenz, I. Marchesini, D. Marconi, M. Meyer, M. Niedziela, D. Nowatschin, J. Ott, F. Pantaleo[15], T. Peiffer, A. Perieanu, N. Pietsch, J. Poehlsen, C. Sander, C. Scharf, P. Schleper, E. Schlieckau, A. Schmidt, S. Schumann, J. Schwandt, H. Stadie, G. Steinbrück, F.M. Stober, H. Tholen, D. Troendle, E. Usai, L. Vanelderen, A. Vanhoefer, B. Vormwald

Institut für Experimentelle Kernphysik, Karlsruhe, Germany
C. Barth, C. Baus, J. Berger, C. Böser, E. Butz, T. Chwalek, F. Colombo, W. De Boer, A. Descroix, A. Dierlamm, S. Fink, F. Frensch, R. Friese, M. Giffels, A. Gilbert, D. Haitz, F. Hartmann[15], S.M. Heindl, U. Husemann, I. Katkov[16], A. Kornmayer[15], P. Lobelle Pardo, B. Maier, H. Mildner, M.U. Mozer, T. Müller, Th. Müller, M. Plagge, G. Quast, K. Rabbertz, S. Röcker, F. Roscher, M. Schröder, G. Sieber, H.J. Simonis, R. Ulrich, J. Wagner-Kuhr, S. Wayand, M. Weber, T. Weiler, S. Williamson, C. Wöhrmann, R. Wolf

Institute of Nuclear and Particle Physics (INPP), NCSR Demokritos, Aghia Paraskevi, Greece
G. Anagnostou, G. Daskalakis, T. Geralis, V.A. Giakoumopoulou, A. Kyriakis, D. Loukas, A. Psallidas, I. Topsis-Giotis

National and Kapodistrian University of Athens, Athens, Greece
A. Agapitos, S. Kesisoglou, A. Panagiotou, N. Saoulidou, E. Tziaferi

University of Ioánnina, Ioánnina, Greece
I. Evangelou, G. Flouris, C. Foudas, P. Kokkas, N. Loukas, N. Manthos, I. Papadopoulos, E. Paradas, J. Strologas

MTA-ELTE Lendület CMS Particle and Nuclear Physics Group, Eötvös Loránd University
N. Filipovic

Wigner Research Centre for Physics, Budapest, Hungary
G. Bencze, C. Hajdu, P. Hidas, D. Horvath[21], F. Sikler, V. Veszpremi, G. Vesztergombi[22], A.J. Zsigmond

Institute of Nuclear Research ATOMKI, Debrecen, Hungary
N. Beni, S. Czellar, J. Karancsi[23], J. Molnar, Z. Szillasi

University of Debrecen, Debrecen, Hungary
M. Bartók[22], A. Makovec, P. Raics, Z.L. Trocsanyi, B. Ujvari

National Institute of Science Education and Research, Bhubaneswar, India
S. Choudhury[24], P. Mal, K. Mandal, A. Nayak, D.K. Sahoo, N. Sahoo, S.K. Swain

Panjab University, Chandigarh, India
S. Bansal, S.B. Beri, V. Bhatnagar, R. Chawla, R. Gupta, U.Bhawandeep, A.K. Kalsi, A. Kaur, M. Kaur, R. Kumar, A. Mehta, M. Mittal, J.B. Singh, G. Walia

University of Delhi, Delhi, India
Ashok Kumar, A. Bhardwaj, B.C. Choudhary, R.B. Garg, S. Keshri, A. Kumar, S. Malhotra, M. Naimuddin, N. Nishu, K. Ranjan, R. Sharma, V. Sharma

Saha Institute of Nuclear Physics, Kolkata, India
R. Bhattacharya, S. Bhattacharya, K. Chatterjee, S. Dey, S. Dutta, S. Ghosh, N. Majumdar, A. Modak, K. Mondal, S. Mukhopadhyay, S. Nandan, A. Purohit, A. Roy, D. Roy, S. Roy Chowdhury, S. Sarkar, M. Sharan

Bhabha Atomic Research Centre, Mumbai, India
R. Chudasama, D. Dutta, V. Jha, V. Kumar, A.K. Mohanty[15], L.M. Pant, P. Shukla, A. Topkar

Tata Institute of Fundamental Research, Mumbai, India
T. Aziz, S. Banerjee, S. Bhowmik[25], R.M. Chatterjee, R.K. Dewanjee, S. Dugad, S. Ganguly, S. Ghosh, M. Guchait, A. Gurtu[26], Sa. Jain, G. Kole, S. Kumar, B. Mahakud, M. Maity[25], G. Majumder, K. Mazumdar, S. Mitra, G.B. Mohanty, B. Parida, T. Sarkar[25], N. Sur, B. Sutar, N. Wickramage[27]

Indian Institute of Science Education and Research (IISER), Pune, India
S. Chauhan, S. Dube, A. Kapoor, K. Kothekar, A. Rane, S. Sharma

Institute for Research in Fundamental Sciences (IPM), Tehran, Iran
H. Bakhshiansohi, H. Behnamian, S.M. Etesami[28], A. Fahim[29], M. Khakzad, M. Mohammadi Najafabadi, M. Naseri, S. Paktinat Mehdiabadi, F. Rezaei Hosseinabadi, B. Safarzadeh[30], M. Zeinali

University College Dublin, Dublin, Ireland
M. Felcini, M. Grunewald

INFN Sezione di Bari ^{a}, Università di Bari ^{b}, Politecnico di Bari ^{c}, Bari, Italy
M. Abbrescia^{a,b}, C. Calabria^{a,b}, C. Caputo^{a,b}, A. Colaleo^a, D. Creanza^{a,c}, L. Cristella^{a,b}, N. De Filippis^{a,c}, M. De Palma^{a,b}, L. Fiore^a, G. Iaselli^{a,c}, G. Maggi^{a,c}, M. Maggi^a, G. Miniello^{a,b}, S. My^{a,b}, S. Nuzzo^{a,b}, A. Pompili^{a,b}, G. Pugliese^{a,c}, R. Radogna^{a,b}, A. Ranieri^a, G. Selvaggi^{a,b}, L. Silvestris^{a,15}, R. Venditti^{a,b}

INFN Sezione di Bologna ^{a}, Università di Bologna ^{b}, Bologna, Italy
G. Abbiendi^a, C. Battilana, D. Bonacorsi^{a,b}, S. Braibant-Giacomelli^{a,b}, L. Brigliadori^{a,b}, R. Campanini^{a,b}, P. Capiluppi^{a,b}, A. Castro^{a,b}, F.R. Cavallo^a, S.S. Chhibra^{a,b}, G. Codispoti^{a,b}, M. Cuffiani^{a,b}, G.M. Dallavalle^a, F. Fabbri^a, A. Fanfani^{a,b}, D. Fasanella^{a,b}, P. Giacomelli^a, C. Grandi^a, L. Guiducci^{a,b}, S. Marcellini^a, G. Masetti^a, A. Montanari^a, F.L. Navarria^{a,b}, A. Perrotta^a, A.M. Rossi^{a,b}, T. Rovelli^{a,b}, G.P. Siroli^{a,b}, N. Tosi^{a,b,15}

INFN Sezione di Catania ^{a}, Università di Catania ^{b}, Catania, Italy
G. Cappello^b, M. Chiorboli^{a,b}, S. Costa^{a,b}, A. Di Mattia^a, F. Giordano^{a,b}, R. Potenza^{a,b}, A. Tricomi^{a,b}, C. Tuve^{a,b}

INFN Sezione di Firenze ^{a}, Università di Firenze ^{b}, Firenze, Italy
G. Barbagli^a, V. Ciulli^{a,b}, C. Civinini^a, R. D'Alessandro^{a,b}, E. Focardi^{a,b}, V. Gori^{a,b}, P. Lenzi^{a,b}, M. Meschini^a, S. Paoletti^a, G. Sguazzoni^a, L. Viliani^{a,b,15}

INFN Laboratori Nazionali di Frascati, Frascati, Italy
L. Benussi, S. Bianco, F. Fabbri, D. Piccolo, F. Primavera[15]

INFN Sezione di Genova ^{a}, Università di Genova ^{b}, Genova, Italy
V. Calvelli^{a,b}, F. Ferro^a, M. Lo Vetere^{a,b}, M.R. Monge^{a,b}, E. Robutti^a, S. Tosi^{a,b}

INFN Sezione di Milano-Bicocca [a]**, Università di Milano-Bicocca** [b]**, Milano, Italy**
L. Brianza, M.E. Dinardo[a,b], S. Fiorendi[a,b], S. Gennai[a], A. Ghezzi[a,b], P. Govoni[a,b], S. Malvezzi[a], R.A. Manzoni[a,b,15], B. Marzocchi[a,b], D. Menasce[a], L. Moroni[a], M. Paganoni[a,b], D. Pedrini[a], S. Pigazzini, S. Ragazzi[a,b], N. Redaelli[a], T. Tabarelli de Fatis[a,b]

INFN Sezione di Napoli [a]**, Università di Napoli 'Federico II'** [b]**, Napoli, Italy, Università della Basilicata** [c]**, Potenza, Italy, Università G. Marconi** [d]**, Roma, Italy**
S. Buontempo[a], N. Cavallo[a,c], S. Di Guida[a,d,15], M. Esposito[a,b], F. Fabozzi[a,c], A.O.M. Iorio[a,b], G. Lanza[a], L. Lista[a], S. Meola[a,d,15], M. Merola[a], P. Paolucci[a,15], C. Sciacca[a,b], F. Thyssen

INFN Sezione di Padova [a]**, Università di Padova** [b]**, Padova, Italy, Università di Trento** [c]**, Trento, Italy**
P. Azzi[a,15], N. Bacchetta[a], M. Bellato[a], L. Benato[a,b], D. Bisello[a,b], A. Boletti[a,b], R. Carlin[a,b], P. Checchia[a], M. Dall'Osso[a,b], P. De Castro Manzano[a], T. Dorigo[a], U. Dosselli[a], S. Fantinel[a], F. Gasparini[a,b], U. Gasparini[a,b], A. Gozzelino[a], S. Lacaprara[a], M. Margoni[a,b], A.T. Meneguzzo[a,b], J. Pazzini[a,b,15], N. Pozzobon[a,b], P. Ronchese[a,b], F. Simonetto[a,b], E. Torassa[a], M. Tosi[a,b], S. Ventura[a], M. Zanetti, P. Zotto[a,b], A. Zucchetta[a,b], G. Zumerle[a,b]

INFN Sezione di Pavia [a]**, Università di Pavia** [b]**, Pavia, Italy**
A. Braghieri[a], A. Magnani[a,b], P. Montagna[a,b], S.P. Ratti[a,b], V. Re[a], C. Riccardi[a,b], P. Salvini[a], I. Vai[a,b], P. Vitulo[a,b]

INFN Sezione di Perugia [a]**, Università di Perugia** [b]**, Perugia, Italy**
L. Alunni Solestizi[a,b], G.M. Bilei[a], D. Ciangottini[a,b], L. Fanò[a,b], P. Lariccia[a,b], R. Leonardi[a,b], G. Mantovani[a,b], M. Menichelli[a], A. Saha[a], A. Santocchia[a,b]

INFN Sezione di Pisa [a]**, Università di Pisa** [b]**, Scuola Normale Superiore di Pisa** [c]**, Pisa, Italy**
K. Androsov[a,31], P. Azzurri[a,15], G. Bagliesi[a], J. Bernardini[a], T. Boccali[a], R. Castaldi[a], M.A. Ciocci[a,31], R. Dell'Orso[a], S. Donato[a,c], G. Fedi, A. Giassi[a], M.T. Grippo[a,31], F. Ligabue[a,c], T. Lomtadze[a], L. Martini[a,b], A. Messineo[a,b], F. Palla[a], A. Rizzi[a,b], A. Savoy-Navarro[a,32], P. Spagnolo[a], R. Tenchini[a], G. Tonelli[a,b], A. Venturi[a], P.G. Verdini[a]

INFN Sezione di Roma [a]**, Università di Roma** [b]**, Roma, Italy**
L. Barone[a,b], F. Cavallari[a], G. D'imperio[a,b,15], D. Del Re[a,b,15], M. Diemoz[a], S. Gelli[a,b], C. Jorda[a], E. Longo[a,b], F. Margaroli[a,b], P. Meridiani[a], G. Organtini[a,b], R. Paramatti[a], F. Preiato[a,b], S. Rahatlou[a,b], C. Rovelli[a], F. Santanastasio[a,b]

INFN Sezione di Torino [a]**, Università di Torino** [b]**, Torino, Italy, Università del Piemonte Orientale** [c]**, Novara, Italy**
N. Amapane[a,b], R. Arcidiacono[a,c,15], S. Argiro[a,b], M. Arneodo[a,c], N. Bartosik[a], R. Bellan[a,b], C. Biino[a], N. Cartiglia[a], M. Costa[a,b], R. Covarelli[a,b], A. Degano[a,b], N. Demaria[a], L. Finco[a,b], B. Kiani[a,b], C. Mariotti[a], S. Maselli[a], E. Migliore[a,b], V. Monaco[a,b], E. Monteil[a,b], M.M. Obertino[a,b], L. Pacher[a,b], N. Pastrone[a], M. Pelliccioni[a], G.L. Pinna Angioni[a,b], F. Ravera[a,b], A. Romero[a,b], M. Ruspa[a,c], R. Sacchi[a,b], V. Sola[a], A. Solano[a,b], A. Staiano[a]

INFN Sezione di Trieste [a]**, Università di Trieste** [b]**, Trieste, Italy**
S. Belforte[a], V. Candelise[a,b], M. Casarsa[a], F. Cossutti[a], G. Della Ricca[a,b], C. La Licata[a,b], A. Schizzi[a,b], A. Zanetti[a]

Kangwon National University, Chunchon, Korea
S.K. Nam

Kyungpook National University, Daegu, Korea
D.H. Kim, G.N. Kim, M.S. Kim, D.J. Kong, S. Lee, S.W. Lee, Y.D. Oh, A. Sakharov, D.C. Son

Chonbuk National University, Jeonju, Korea
J.A. Brochero Cifuentes, H. Kim, T.J. Kim[33]

Chonnam National University, Institute for Universe and Elementary Particles, Kwangju, Korea
S. Song

Korea University, Seoul, Korea
S. Cho, S. Choi, Y. Go, D. Gyun, B. Hong, Y. Kim, B. Lee, K. Lee, K.S. Lee, S. Lee, J. Lim, S.K. Park, Y. Roh

Seoul National University, Seoul, Korea
H.D. Yoo

University of Seoul, Seoul, Korea
M. Choi, H. Kim, H. Kim, J.H. Kim, J.S.H. Lee, I.C. Park, G. Ryu, M.S. Ryu

Sungkyunkwan University, Suwon, Korea
Y. Choi, J. Goh, D. Kim, E. Kwon, J. Lee, I. Yu

Vilnius University, Vilnius, Lithuania
V. Dudenas, A. Juodagalvis, J. Vaitkus

National Centre for Particle Physics, Universiti Malaya, Kuala Lumpur, Malaysia
I. Ahmed, Z.A. Ibrahim, J.R. Komaragiri, M.A.B. Md Ali[34], F. Mohamad Idris[35], W.A.T. Wan Abdullah, M.N. Yusli, Z. Zolkapli

Centro de Investigacion y de Estudios Avanzados del IPN, Mexico City, Mexico
E. Casimiro Linares, H. Castilla-Valdez, E. De La Cruz-Burelo, I. Heredia-De La Cruz[36], A. Hernandez-Almada, R. Lopez-Fernandez, J. Mejia Guisao, A. Sanchez-Hernandez

Universidad Iberoamericana, Mexico City, Mexico
S. Carrillo Moreno, F. Vazquez Valencia

Benemerita Universidad Autonoma de Puebla, Puebla, Mexico
I. Pedraza, H.A. Salazar Ibarguen, C. Uribe Estrada

Universidad Autónoma de San Luis Potosí, San Luis Potosí, Mexico
A. Morelos Pineda

University of Auckland, Auckland, New Zealand
D. Krofcheck

University of Canterbury, Christchurch, New Zealand
P.H. Butler

National Centre for Physics, Quaid-I-Azam University, Islamabad, Pakistan
A. Ahmad, M. Ahmad, Q. Hassan, H.R. Hoorani, W.A. Khan, T. Khurshid, M. Shoaib, M. Waqas

National Centre for Nuclear Research, Swierk, Poland
H. Bialkowska, M. Bluj, B. Boimska, T. Frueboes, M. Górski, M. Kazana, K. Nawrocki, K. Romanowska-Rybinska, M. Szleper, P. Traczyk, P. Zalewski

Institute of Experimental Physics, Faculty of Physics, University of Warsaw, Warsaw, Poland
G. Brona, K. Bunkowski, A. Byszuk[37], K. Doroba, A. Kalinowski, M. Konecki, J. Krolikowski, M. Misiura, M. Olszewski, M. Walczak

Laboratório de Instrumentação e Física Experimental de Partículas, Lisboa, Portugal
P. Bargassa, C. Beirão Da Cruz E Silva, A. Di Francesco, P. Faccioli, P.G. Ferreira Parracho, M. Gallinaro, J. Hollar, N. Leonardo, L. Lloret Iglesias, M.V. Nemallapudi, F. Nguyen, J. Rodrigues Antunes, J. Seixas, O. Toldaiev, D. Vadruccio, J. Varela, P. Vischia

Joint Institute for Nuclear Research, Dubna, Russia
P. Bunin, I. Golutvin, A. Kamenev, V. Karjavin, V. Korenkov, A. Lanev, A. Malakhov, V. Matveev[38,39], V.V. Mitsyn, P. Moisenz, V. Palichik, V. Perelygin, S. Shmatov, S. Shulha, N. Skatchkov, V. Smirnov, E. Tikhonenko, N. Voytishin, A. Zarubin

Petersburg Nuclear Physics Institute, Gatchina (St. Petersburg), Russia
V. Golovtsov, Y. Ivanov, V. Kim[40], E. Kuznetsova[41], P. Levchenko, V. Murzin, V. Oreshkin, I. Smirnov, V. Sulimov, L. Uvarov, S. Vavilov, A. Vorobyev

Institute for Nuclear Research, Moscow, Russia
Yu. Andreev, A. Dermenev, S. Gninenko, N. Golubev, A. Karneyeu, M. Kirsanov, N. Krasnikov, A. Pashenkov, D. Tlisov, A. Toropin

Institute for Theoretical and Experimental Physics, Moscow, Russia
V. Epshteyn, V. Gavrilov, N. Lychkovskaya, V. Popov, I. Pozdnyakov, G. Safronov, A. Spiridonov, M. Toms, E. Vlasov, A. Zhokin

National Research Nuclear University 'Moscow Engineering Physics Institute' (MEPhI), Moscow, Russia
M. Chadeeva, R. Chistov, M. Danilov, V. Rusinov, E. Tarkovskii

P.N. Lebedev Physical Institute, Moscow, Russia
V. Andreev, M. Azarkin[39], I. Dremin[39], M. Kirakosyan, A. Leonidov[39], G. Mesyats, S.V. Rusakov

Skobeltsyn Institute of Nuclear Physics, Lomonosov Moscow State University, Moscow, Russia
A. Baskakov, A. Belyaev, E. Boos, V. Bunichev, M. Dubinin[42], L. Dudko, A. Ershov, V. Klyukhin, N. Korneeva, I. Lokhtin, I. Miagkov, S. Obraztsov, M. Perfilov, S. Petrushanko, V. Savrin

State Research Center of Russian Federation, Institute for High Energy Physics, Protvino, Russia
I. Azhgirey, I. Bayshev, S. Bitioukov, V. Kachanov, A. Kalinin, D. Konstantinov, V. Krychkine, V. Petrov, R. Ryutin, A. Sobol, L. Tourtchanovitch, S. Troshin, N. Tyurin, A. Uzunian, A. Volkov

University of Belgrade, Faculty of Physics and Vinca Institute of Nuclear Sciences, Belgrade, Serbia
P. Adzic[43], P. Cirkovic, D. Devetak, J. Milosevic, V. Rekovic

Centro de Investigaciones Energéticas Medioambientales y Tecnológicas (CIEMAT), Madrid, Spain
J. Alcaraz Maestre, E. Calvo, M. Cerrada, M. Chamizo Llatas, N. Colino, B. De La Cruz, A. Delgado Peris, A. Escalante Del Valle, C. Fernandez Bedoya, J.P. Fernández Ramos, J. Flix, M.C. Fouz, P. Garcia-Abia, O. Gonzalez Lopez, S. Goy Lopez, J.M. Hernandez, M.I. Josa, E. Navarro De Martino, A. Pérez-Calero Yzquierdo, J. Puerta Pelayo, A. Quintario Olmeda, I. Redondo, L. Romero, M.S. Soares

Universidad Autónoma de Madrid, Madrid, Spain
J.F. de Trocóniz, M. Missiroli, D. Moran

Universidad de Oviedo, Oviedo, Spain
J. Cuevas, J. Fernandez Menendez, S. Folgueras, I. Gonzalez Caballero, E. Palencia Cortezon, J.M. Vizan Garcia

Instituto de Física de Cantabria (IFCA), CSIC-Universidad de Cantabria, Santander, Spain
I.J. Cabrillo, A. Calderon, J.R. Castiñeiras De Saa, E. Curras, M. Fernandez, J. Garcia-Ferrero, G. Gomez, A. Lopez Virto, J. Marco, R. Marco, C. Martinez Rivero, F. Matorras, J. Piedra Gomez, T. Rodrigo, A.Y. Rodríguez-Marrero, A. Ruiz-Jimeno, L. Scodellaro, N. Trevisani, I. Vila, R. Vilar Cortabitarte

CERN, European Organization for Nuclear Research, Geneva, Switzerland
D. Abbaneo, E. Auffray, G. Auzinger, M. Bachtis, P. Baillon, A.H. Ball, D. Barney, A. Benaglia, L. Benhabib, G.M. Berruti, P. Bloch, A. Bocci, A. Bonato, C. Botta, H. Breuker, T. Camporesi, R. Castello, M. Cepeda, G. Cerminara, M. D'Alfonso, D. d'Enterria, A. Dabrowski, V. Daponte, A. David, M. De Gruttola, F. De Guio, A. De Roeck, E. Di Marco[44], M. Dobson, M. Dordevic, B. Dorney, T. du Pree, D. Duggan, M. Dünser, N. Dupont, A. Elliott-Peisert, S. Fartoukh, G. Franzoni, J. Fulcher, W. Funk, D. Gigi, K. Gill, M. Girone, F. Glege, R. Guida, S. Gundacker, M. Guthoff, J. Hammer, P. Harris, J. Hegeman, V. Innocente, P. Janot, H. Kirschenmann, V. Knünz, M.J. Kortelainen, K. Kousouris, P. Lecoq, C. Lourenço, M.T. Lucchini, N. Magini, L. Malgeri, M. Mannelli, A. Martelli, L. Masetti, F. Meijers, S. Mersi, E. Meschi, F. Moortgat, S. Morovic, M. Mulders, H. Neugebauer, S. Orfanelli[45], L. Orsini, L. Pape, E. Perez, M. Peruzzi, A. Petrilli, G. Petrucciani, A. Pfeiffer, M. Pierini, D. Piparo, A. Racz, T. Reis, G. Rolandi[46], M. Rovere, M. Ruan, H. Sakulin, J.B. Sauvan, C. Schäfer, C. Schwick, M. Seidel, A. Sharma, P. Silva, M. Simon, P. Sphicas[47], J. Steggemann, M. Stoye, Y. Takahashi, D. Treille, A. Triossi, A. Tsirou, V. Veckalns[48], G.I. Veres[22], N. Wardle, H.K. Wöhri, A. Zagozdzinska[37], W.D. Zeuner

Paul Scherrer Institut, Villigen, Switzerland
W. Bertl, K. Deiters, W. Erdmann, R. Horisberger, Q. Ingram, H.C. Kaestli, D. Kotlinski, U. Langenegger, T. Rohe

Institute for Particle Physics, ETH Zurich, Zurich, Switzerland
F. Bachmair, L. Bäni, L. Bianchini, B. Casal, G. Dissertori, M. Dittmar, M. Donegà, P. Eller, C. Grab, C. Heidegger, D. Hits, J. Hoss, G. Kasieczka, P. Lecomte[†], W. Lustermann, B. Mangano, M. Marionneau, P. Martinez Ruiz del Arbol, M. Masciovecchio, M.T. Meinhard, D. Meister, F. Micheli, P. Musella, F. Nessi-Tedaldi, F. Pandolfi, J. Pata, F. Pauss, G. Perrin, L. Perrozzi, M. Quittnat, M. Rossini, M. Schönenberger, A. Starodumov[49], M. Takahashi, V.R. Tavolaro, K. Theofilatos, R. Wallny

Universität Zürich, Zurich, Switzerland
T.K. Aarrestad, C. Amsler[50], L. Caminada, M.F. Canelli, V. Chiochia, A. De Cosa, C. Galloni, A. Hinzmann, T. Hreus, B. Kilminster, C. Lange, J. Ngadiuba, D. Pinna, G. Rauco, P. Robmann, D. Salerno, Y. Yang

National Central University, Chung-Li, Taiwan
K.H. Chen, T.H. Doan, Sh. Jain, R. Khurana, M. Konyushikhin, C.M. Kuo, W. Lin, Y.J. Lu, A. Pozdnyakov, S.S. Yu

National Taiwan University (NTU), Taipei, Taiwan
Arun Kumar, P. Chang, Y.H. Chang, Y.W. Chang, Y. Chao, K.F. Chen, P.H. Chen, C. Dietz, F. Fiori, W.-S. Hou, Y. Hsiung, Y.F. Liu, R.-S. Lu, M. Miñano Moya, J.f. Tsai, Y.M. Tzeng

Chulalongkorn University, Faculty of Science, Department of Physics, Bangkok, Thailand
B. Asavapibhop, K. Kovitanggoon, G. Singh, N. Srimanobhas, N. Suwonjandee

Cukurova University, Adana, Turkey
A. Adiguzel, S. Cerci[51], S. Damarseckin, Z.S. Demiroglu, C. Dozen, I. Dumanoglu, S. Girgis, G. Gokbulut, Y. Guler, E. Gurpinar, I. Hos, E.E. Kangal[52], A. Kayis Topaksu, G. Onengut[53], K. Ozdemir[54], S. Ozturk[55], B. Tali[51], H. Topakli[55], C. Zorbilmez

Middle East Technical University, Physics Department, Ankara, Turkey
B. Bilin, S. Bilmis, B. Isildak[56], G. Karapinar[57], M. Yalvac, M. Zeyrek

Bogazici University, Istanbul, Turkey
E. Gülmez, M. Kaya[58], O. Kaya[59], E.A. Yetkin[60], T. Yetkin[61]

Istanbul Technical University, Istanbul, Turkey
A. Cakir, K. Cankocak, S. Sen[62], F.I. Vardarlı

Institute for Scintillation Materials of National Academy of Science of Ukraine, Kharkov, Ukraine
B. Grynyov

National Scientific Center, Kharkov Institute of Physics and Technology, Kharkov, Ukraine
L. Levchuk, P. Sorokin

University of Bristol, Bristol, United Kingdom
R. Aggleton, F. Ball, L. Beck, J.J. Brooke, D. Burns, E. Clement, D. Cussans, H. Flacher, J. Goldstein, M. Grimes, G.P. Heath, H.F. Heath, J. Jacob, L. Kreczko, C. Lucas, Z. Meng, D.M. Newbold[63], S. Paramesvaran, A. Poll, T. Sakuma, S. Seif El Nasr-storey, S. Senkin, D. Smith, V.J. Smith

Rutherford Appleton Laboratory, Didcot, United Kingdom
K.W. Bell, A. Belyaev[64], C. Brew, R.M. Brown, L. Calligaris, D. Cieri, D.J.A. Cockerill, J.A. Coughlan, K. Harder, S. Harper, E. Olaiya, D. Petyt, C.H. Shepherd-Themistocleous, A. Thea, I.R. Tomalin, T. Williams, S.D. Worm

Imperial College, London, United Kingdom
M. Baber, R. Bainbridge, O. Buchmuller, A. Bundock, D. Burton, S. Casasso, M. Citron, D. Colling, L. Corpe, P. Dauncey, G. Davies, A. De Wit, M. Della Negra, P. Dunne, A. Elwood, D. Futyan, Y. Haddad, G. Hall, G. Iles, R. Lane, R. Lucas[63], L. Lyons, A.-M. Magnan, S. Malik, L. Mastrolorenzo, J. Nash, A. Nikitenko[49], J. Pela, B. Penning, M. Pesaresi, D.M. Raymond, A. Richards, A. Rose, C. Seez, A. Tapper, K. Uchida, M. Vazquez Acosta[65], T. Virdee[15], S.C. Zenz

Brunel University, Uxbridge, United Kingdom
J.E. Cole, P.R. Hobson, A. Khan, P. Kyberd, D. Leslie, I.D. Reid, P. Symonds, L. Teodorescu, M. Turner

Baylor University, Waco, USA
A. Borzou, K. Call, J. Dittmann, K. Hatakeyama, H. Liu, N. Pastika

The University of Alabama, Tuscaloosa, USA
O. Charaf, S.I. Cooper, C. Henderson, P. Rumerio

Boston University, Boston, USA
D. Arcaro, A. Avetisyan, T. Bose, D. Gastler, D. Rankin, C. Richardson, J. Rohlf, L. Sulak, D. Zou

Brown University, Providence, USA
J. Alimena, G. Benelli, E. Berry, D. Cutts, A. Ferapontov, A. Garabedian, J. Hakala, U. Heintz, O. Jesus, E. Laird, G. Landsberg, Z. Mao, M. Narain, S. Piperov, S. Sagir, R. Syarif

University of California, Davis, Davis, USA

R. Breedon, G. Breto, M. Calderon De La Barca Sanchez, S. Chauhan, M. Chertok, J. Conway, R. Conway, P.T. Cox, R. Erbacher, G. Funk, M. Gardner, W. Ko, R. Lander, C. Mclean, M. Mulhearn, D. Pellett, J. Pilot, F. Ricci-Tam, S. Shalhout, J. Smith, M. Squires, D. Stolp, M. Tripathi, S. Wilbur, R. Yohay

University of California, Los Angeles, USA

R. Cousins, P. Everaerts, A. Florent, J. Hauser, M. Ignatenko, D. Saltzberg, E. Takasugi, V. Valuev, M. Weber

University of California, Riverside, Riverside, USA

K. Burt, R. Clare, J. Ellison, J.W. Gary, G. Hanson, J. Heilman, M. Ivova PANEVA, P. Jandir, E. Kennedy, F. Lacroix, O.R. Long, M. Malberti, M. Olmedo Negrete, A. Shrinivas, H. Wei, S. Wimpenny, B. R. Yates

University of California, San Diego, La Jolla, USA

J.G. Branson, G.B. Cerati, S. Cittolin, R.T. D'Agnolo, M. Derdzinski, R. Gerosa, A. Holzner, R. Kelley, D. Klein, J. Letts, I. Macneill, D. Olivito, S. Padhi, M. Pieri, M. Sani, V. Sharma, S. Simon, M. Tadel, A. Vartak, S. Wasserbaech[66], C. Welke, J. Wood, F. Würthwein, A. Yagil, G. Zevi Della Porta

University of California, Santa Barbara, Santa Barbara, USA

J. Bradmiller-Feld, C. Campagnari, A. Dishaw, V. Dutta, K. Flowers, M. Franco Sevilla, P. Geffert, C. George, F. Golf, L. Gouskos, J. Gran, J. Incandela, N. Mccoll, S.D. Mullin, J. Richman, D. Stuart, I. Suarez, C. West, J. Yoo

California Institute of Technology, Pasadena, USA

D. Anderson, A. Apresyan, J. Bendavid, A. Bornheim, J. Bunn, Y. Chen, J. Duarte, A. Mott, H.B. Newman, C. Pena, M. Spiropulu, J.R. Vlimant, S. Xie, R.Y. Zhu

Carnegie Mellon University, Pittsburgh, USA

M.B. Andrews, V. Azzolini, A. Calamba, B. Carlson, T. Ferguson, M. Paulini, J. Russ, M. Sun, H. Vogel, I. Vorobiev

University of Colorado Boulder, Boulder, USA

J.P. Cumalat, W.T. Ford, F. Jensen, A. Johnson, M. Krohn, T. Mulholland, U. Nauenberg, K. Stenson, S.R. Wagner

Cornell University, Ithaca, USA

J. Alexander, A. Chatterjee, J. Chaves, J. Chu, S. Dittmer, N. Eggert, N. Mirman, G. Nicolas Kaufman, J.R. Patterson, A. Rinkevicius, A. Ryd, L. Skinnari, L. Soffi, W. Sun, S.M. Tan, W.D. Teo, J. Thom, J. Thompson, J. Tucker, Y. Weng, P. Wittich

Fermi National Accelerator Laboratory, Batavia, USA

S. Abdullin, M. Albrow, G. Apollinari, S. Banerjee, L.A.T. Bauerdick, A. Beretvas, J. Berryhill, P.C. Bhat, G. Bolla, K. Burkett, J.N. Butler, H.W.K. Cheung, F. Chlebana, S. Cihangir, V.D. Elvira, I. Fisk, J. Freeman, E. Gottschalk, L. Gray, D. Green, S. Grünendahl, O. Gutsche, J. Hanlon, D. Hare, R.M. Harris, S. Hasegawa, J. Hirschauer, Z. Hu, B. Jayatilaka, S. Jindariani, M. Johnson, U. Joshi, B. Klima, B. Kreis, S. Lammel, J. Lewis, J. Linacre, D. Lincoln, R. Lipton, T. Liu, R. Lopes De Sá, J. Lykken, K. Maeshima, J.M. Marraffino, S. Maruyama, D. Mason, P. McBride, P. Merkel, S. Mrenna, S. Nahn, C. Newman-Holmes[†], V. O'Dell, K. Pedro, O. Prokofyev, G. Rakness, E. Sexton-Kennedy, A. Soha, W.J. Spalding, L. Spiegel, S. Stoynev, N. Strobbe, L. Taylor, S. Tkaczyk, N.V. Tran, L. Uplegger, E.W. Vaandering, C. Vernieri, M. Verzocchi, R. Vidal, M. Wang, H.A. Weber, A. Whitbeck

University of Florida, Gainesville, USA
D. Acosta, P. Avery, P. Bortignon, D. Bourilkov, A. Brinkerhoff, A. Carnes, M. Carver, D. Curry, S. Das, R.D. Field, I.K. Furic, J. Konigsberg, A. Korytov, K. Kotov, P. Ma, K. Matchev, H. Mei, P. Milenovic[67], G. Mitselmakher, D. Rank, R. Rossin, L. Shchutska, D. Sperka, N. Terentyev, L. Thomas, J. Wang, S. Wang, J. Yelton

Florida International University, Miami, USA
S. Linn, P. Markowitz, G. Martinez, J.L. Rodriguez

Florida State University, Tallahassee, USA
A. Ackert, J.R. Adams, T. Adams, A. Askew, S. Bein, J. Bochenek, B. Diamond, J. Haas, S. Hagopian, V. Hagopian, K.F. Johnson, A. Khatiwada, H. Prosper, A. Santra, M. Weinberg

Florida Institute of Technology, Melbourne, USA
M.M. Baarmand, V. Bhopatkar, S. Colafranceschi[68], M. Hohlmann, H. Kalakhety, D. Noonan, T. Roy, F. Yumiceva

University of Illinois at Chicago (UIC), Chicago, USA
M.R. Adams, L. Apanasevich, D. Berry, R.R. Betts, I. Bucinskaite, R. Cavanaugh, O. Evdokimov, L. Gauthier, C.E. Gerber, D.J. Hofman, P. Kurt, C. O'Brien, I.D. Sandoval Gonzalez, P. Turner, N. Varelas, Z. Wu, M. Zakaria, J. Zhang

The University of Iowa, Iowa City, USA
B. Bilki[69], W. Clarida, K. Dilsiz, S. Durgut, R.P. Gandrajula, M. Haytmyradov, V. Khristenko, J.-P. Merlo, H. Mermerkaya[70], A. Mestvirishvili, A. Moeller, J. Nachtman, H. Ogul, Y. Onel, F. Ozok[71], A. Penzo, C. Snyder, E. Tiras, J. Wetzel, K. Yi

Johns Hopkins University, Baltimore, USA
I. Anderson, B. Blumenfeld, A. Cocoros, N. Eminizer, D. Fehling, L. Feng, A.V. Gritsan, P. Maksimovic, M. Osherson, J. Roskes, U. Sarica, M. Swartz, M. Xiao, Y. Xin, C. You

The University of Kansas, Lawrence, USA
P. Baringer, A. Bean, C. Bruner, J. Castle, R.P. Kenny III, A. Kropivnitskaya, D. Majumder, M. Malek, W. Mcbrayer, M. Murray, S. Sanders, R. Stringer, Q. Wang

Kansas State University, Manhattan, USA
A. Ivanov, K. Kaadze, S. Khalil, M. Makouski, Y. Maravin, A. Mohammadi, L.K. Saini, N. Skhirtladze, S. Toda

Lawrence Livermore National Laboratory, Livermore, USA
D. Lange, F. Rebassoo, D. Wright

University of Maryland, College Park, USA
C. Anelli, A. Baden, O. Baron, A. Belloni, B. Calvert, S.C. Eno, C. Ferraioli, J.A. Gomez, N.J. Hadley, S. Jabeen, R.G. Kellogg, T. Kolberg, J. Kunkle, Y. Lu, A.C. Mignerey, Y.H. Shin, A. Skuja, M.B. Tonjes, S.C. Tonwar

Massachusetts Institute of Technology, Cambridge, USA
A. Apyan, R. Barbieri, A. Baty, R. Bi, K. Bierwagen, S. Brandt, W. Busza, I.A. Cali, Z. Demiragli, L. Di Matteo, G. Gomez Ceballos, M. Goncharov, D. Gulhan, D. Hsu, Y. Iiyama, G.M. Innocenti, M. Klute, D. Kovalskyi, K. Krajczar, Y.S. Lai, Y.-J. Lee, A. Levin, P.D. Luckey, A.C. Marini, C. Mcginn, C. Mironov, S. Narayanan, X. Niu, C. Paus, C. Roland, G. Roland, J. Salfeld-Nebgen, G.S.F. Stephans, K. Sumorok, K. Tatar, M. Varma, D. Velicanu, J. Veverka, J. Wang, T.W. Wang, B. Wyslouch, M. Yang, V. Zhukova

University of Minnesota, Minneapolis, USA
A.C. Benvenuti, B. Dahmes, A. Evans, A. Finkel, A. Gude, P. Hansen, S. Kalafut, S.C. Kao, K. Klapoetke, Y. Kubota, Z. Lesko, J. Mans, S. Nourbakhsh, N. Ruckstuhl, R. Rusack, N. Tambe, J. Turkewitz

University of Mississippi, Oxford, USA
J.G. Acosta, S. Oliveros

University of Nebraska-Lincoln, Lincoln, USA
E. Avdeeva, R. Bartek, K. Bloom, S. Bose, D.R. Claes, A. Dominguez, C. Fangmeier, R. Gonzalez Suarez, R. Kamalieddin, D. Knowlton, I. Kravchenko, F. Meier, J. Monroy, F. Ratnikov, J.E. Siado, G.R. Snow, B. Stieger

State University of New York at Buffalo, Buffalo, USA
M. Alyari, J. Dolen, J. George, A. Godshalk, C. Harrington, I. Iashvili, J. Kaisen, A. Kharchilava, A. Kumar, A. Parker, S. Rappoccio, B. Roozbahani

Northeastern University, Boston, USA
G. Alverson, E. Barberis, D. Baumgartel, M. Chasco, A. Hortiangtham, A. Massironi, D.M. Morse, D. Nash, T. Orimoto, R. Teixeira De Lima, D. Trocino, R.-J. Wang, D. Wood, J. Zhang

Northwestern University, Evanston, USA
S. Bhattacharya, K.A. Hahn, A. Kubik, J.F. Low, N. Mucia, N. Odell, B. Pollack, M.H. Schmitt, K. Sung, M. Trovato, M. Velasco

University of Notre Dame, Notre Dame, USA
N. Dev, M. Hildreth, C. Jessop, D.J. Karmgard, N. Kellams, K. Lannon, N. Marinelli, F. Meng, C. Mueller, Y. Musienko[38], M. Planer, A. Reinsvold, R. Ruchti, N. Rupprecht, G. Smith, S. Taroni, N. Valls, M. Wayne, M. Wolf, A. Woodard

The Ohio State University, Columbus, USA
L. Antonelli, J. Brinson, B. Bylsma, L.S. Durkin, S. Flowers, A. Hart, C. Hill, R. Hughes, W. Ji, T.Y. Ling, B. Liu, W. Luo, D. Puigh, M. Rodenburg, B.L. Winer, H.W. Wulsin

Princeton University, Princeton, USA
O. Driga, P. Elmer, J. Hardenbrook, P. Hebda, S.A. Koay, P. Lujan, D. Marlow, T. Medvedeva, M. Mooney, J. Olsen, C. Palmer, P. Piroué, D. Stickland, C. Tully, A. Zuranski

University of Puerto Rico, Mayaguez, USA
S. Malik

Purdue University, West Lafayette, USA
A. Barker, V.E. Barnes, D. Benedetti, L. Gutay, M.K. Jha, M. Jones, A.W. Jung, K. Jung, D.H. Miller, N. Neumeister, B.C. Radburn-Smith, X. Shi, J. Sun, A. Svyatkovskiy, F. Wang, W. Xie, L. Xu

Purdue University Calumet, Hammond, USA
N. Parashar, J. Stupak

Rice University, Houston, USA
A. Adair, B. Akgun, Z. Chen, K.M. Ecklund, F.J.M. Geurts, M. Guilbaud, W. Li, B. Michlin, M. Northup, B.P. Padley, R. Redjimi, J. Roberts, J. Rorie, Z. Tu, J. Zabel

University of Rochester, Rochester, USA
B. Betchart, A. Bodek, P. de Barbaro, R. Demina, Y.t. Duh, Y. Eshaq, T. Ferbel, M. Galanti,
A. Garcia-Bellido, J. Han, O. Hindrichs, A. Khukhunaishvili, K.H. Lo, P. Tan, M. Verzetti

Rutgers, The State University of New Jersey, Piscataway, USA
J.P. Chou, E. Contreras-Campana, Y. Gershtein, T.A. Gómez Espinosa, E. Halkiadakis,
M. Heindl, D. Hidas, E. Hughes, S. Kaplan, R. Kunnawalkam Elayavalli, S. Kyriacou, A. Lath,
K. Nash, H. Saka, S. Salur, S. Schnetzer, D. Sheffield, S. Somalwar, R. Stone, S. Thomas,
P. Thomassen, M. Walker

University of Tennessee, Knoxville, USA
M. Foerster, J. Heideman, G. Riley, K. Rose, S. Spanier, K. Thapa

Texas A&M University, College Station, USA
O. Bouhali[72], A. Castaneda Hernandez[72], A. Celik, M. Dalchenko, M. De Mattia, A. Delgado,
S. Dildick, R. Eusebi, J. Gilmore, T. Huang, T. Kamon[73], V. Krutelyov, R. Mueller, I. Osipenkov,
Y. Pakhotin, R. Patel, A. Perloff, L. Perniè, D. Rathjens, A. Rose, A. Safonov, A. Tatarinov,
K.A. Ulmer

Texas Tech University, Lubbock, USA
N. Akchurin, C. Cowden, J. Damgov, C. Dragoiu, P.R. Dudero, J. Faulkner, S. Kunori,
K. Lamichhane, S.W. Lee, T. Libeiro, S. Undleeb, I. Volobouev, Z. Wang

Vanderbilt University, Nashville, USA
E. Appelt, A.G. Delannoy, S. Greene, A. Gurrola, R. Janjam, W. Johns, C. Maguire, Y. Mao,
A. Melo, H. Ni, P. Sheldon, S. Tuo, J. Velkovska, Q. Xu

University of Virginia, Charlottesville, USA
M.W. Arenton, P. Barria, B. Cox, B. Francis, J. Goodell, R. Hirosky, A. Ledovskoy, H. Li, C. Neu,
T. Sinthuprasith, X. Sun, Y. Wang, E. Wolfe, F. Xia

Wayne State University, Detroit, USA
C. Clarke, R. Harr, P.E. Karchin, C. Kottachchi Kankanamge Don, P. Lamichhane, J. Sturdy

University of Wisconsin - Madison, Madison, WI, USA
D.A. Belknap, D. Carlsmith, S. Dasu, L. Dodd, S. Duric, B. Gomber, M. Grothe, M. Herndon,
A. Hervé, P. Klabbers, A. Lanaro, A. Levine, K. Long, R. Loveless, A. Mohapatra, I. Ojalvo,
T. Perry, G.A. Pierro, G. Polese, T. Ruggles, T. Sarangi, A. Savin, A. Sharma, N. Smith,
W.H. Smith, D. Taylor, P. Verwilligen, N. Woods

†: Deceased
1: Also at Vienna University of Technology, Vienna, Austria
2: Also at State Key Laboratory of Nuclear Physics and Technology, Peking University, Beijing,
China
3: Also at Institut Pluridisciplinaire Hubert Curien, Université de Strasbourg, Université de
Haute Alsace Mulhouse, CNRS/IN2P3, Strasbourg, France
4: Also at Universidade Estadual de Campinas, Campinas, Brazil
5: Also at Centre National de la Recherche Scientifique (CNRS) - IN2P3, Paris, France
6: Also at Université Libre de Bruxelles, Bruxelles, Belgium
7: Also at Laboratoire Leprince-Ringuet, Ecole Polytechnique, IN2P3-CNRS, Palaiseau, France
8: Also at Joint Institute for Nuclear Research, Dubna, Russia
9: Also at Suez University, Suez, Egypt
10: Now at British University in Egypt, Cairo, Egypt
11: Also at Cairo University, Cairo, Egypt

12: Now at Helwan University, Cairo, Egypt
13: Now at Ain Shams University, Cairo, Egypt
14: Also at Université de Haute Alsace, Mulhouse, France
15: Also at CERN, European Organization for Nuclear Research, Geneva, Switzerland
16: Also at Skobeltsyn Institute of Nuclear Physics, Lomonosov Moscow State University, Moscow, Russia
17: Also at Tbilisi State University, Tbilisi, Georgia
18: Also at RWTH Aachen University, III. Physikalisches Institut A, Aachen, Germany
19: Also at University of Hamburg, Hamburg, Germany
20: Also at Brandenburg University of Technology, Cottbus, Germany
21: Also at Institute of Nuclear Research ATOMKI, Debrecen, Hungary
22: Also at MTA-ELTE Lendület CMS Particle and Nuclear Physics Group, Eötvös Loránd University, Budapest, Hungary
23: Also at University of Debrecen, Debrecen, Hungary
24: Also at Indian Institute of Science Education and Research, Bhopal, India
25: Also at University of Visva-Bharati, Santiniketan, India
26: Now at King Abdulaziz University, Jeddah, Saudi Arabia
27: Also at University of Ruhuna, Matara, Sri Lanka
28: Also at Isfahan University of Technology, Isfahan, Iran
29: Also at University of Tehran, Department of Engineering Science, Tehran, Iran
30: Also at Plasma Physics Research Center, Science and Research Branch, Islamic Azad University, Tehran, Iran
31: Also at Università degli Studi di Siena, Siena, Italy
32: Also at Purdue University, West Lafayette, USA
33: Now at Hanyang University, Seoul, Korea
34: Also at International Islamic University of Malaysia, Kuala Lumpur, Malaysia
35: Also at Malaysian Nuclear Agency, MOSTI, Kajang, Malaysia
36: Also at Consejo Nacional de Ciencia y Tecnología, Mexico city, Mexico
37: Also at Warsaw University of Technology, Institute of Electronic Systems, Warsaw, Poland
38: Also at Institute for Nuclear Research, Moscow, Russia
39: Now at National Research Nuclear University 'Moscow Engineering Physics Institute' (MEPhI), Moscow, Russia
40: Also at St. Petersburg State Polytechnical University, St. Petersburg, Russia
41: Also at University of Florida, Gainesville, USA
42: Also at California Institute of Technology, Pasadena, USA
43: Also at Faculty of Physics, University of Belgrade, Belgrade, Serbia
44: Also at INFN Sezione di Roma; Università di Roma, Roma, Italy
45: Also at National Technical University of Athens, Athens, Greece
46: Also at Scuola Normale e Sezione dell'INFN, Pisa, Italy
47: Also at National and Kapodistrian University of Athens, Athens, Greece
48: Also at Riga Technical University, Riga, Latvia
49: Also at Institute for Theoretical and Experimental Physics, Moscow, Russia
50: Also at Albert Einstein Center for Fundamental Physics, Bern, Switzerland
51: Also at Adiyaman University, Adiyaman, Turkey
52: Also at Mersin University, Mersin, Turkey
53: Also at Cag University, Mersin, Turkey
54: Also at Piri Reis University, Istanbul, Turkey
55: Also at Gaziosmanpasa University, Tokat, Turkey
56: Also at Ozyegin University, Istanbul, Turkey

57: Also at Izmir Institute of Technology, Izmir, Turkey

58: Also at Marmara University, Istanbul, Turkey

59: Also at Kafkas University, Kars, Turkey

60: Also at Istanbul Bilgi University, Istanbul, Turkey

61: Also at Yildiz Technical University, Istanbul, Turkey

62: Also at Hacettepe University, Ankara, Turkey

63: Also at Rutherford Appleton Laboratory, Didcot, United Kingdom

64: Also at School of Physics and Astronomy, University of Southampton, Southampton, United Kingdom

65: Also at Instituto de Astrofísica de Canarias, La Laguna, Spain

66: Also at Utah Valley University, Orem, USA

67: Also at University of Belgrade, Faculty of Physics and Vinca Institute of Nuclear Sciences, Belgrade, Serbia

68: Also at Facoltà Ingegneria, Università di Roma, Roma, Italy

69: Also at Argonne National Laboratory, Argonne, USA

70: Also at Erzincan University, Erzincan, Turkey

71: Also at Mimar Sinan University, Istanbul, Istanbul, Turkey

72: Also at Texas A&M University at Qatar, Doha, Qatar

73: Also at Kyungpook National University, Daegu, Korea